Turkish Journal of Earth Sciences

http://journals.tubitak.gov.tr/earth/

Research Article

Turkish J Earth Sci
(2020) 29: 28-63
© TÜBİTAK
doi:10.3906/yer-1907-7

Biostratigraphy and paleoenvironments of the Oligocene succession (İhsaniye Formation) at Karaburun (NW Turkey)

Michael D. SIMMONS[1,2,*], Michael D. BIDGOOD[3], Paul G. CONNELL[4], Stjepan ĆORIĆ[5], Aral I. OKAY[6], David SHAW[7], Emilia TULAN[8], Jan MAYER[9], Gabor C. TARI[10]

[1]The Natural History Museum, London, UK
[2]Halliburton, Milton Park, Abingdon, UK
[3]GSS (Geoscience) Ltd, Oldmeldrum, Aberdeenshire, UK
[4]8 Leslie Crescent, Aberdeenshire, UK
[5]Geological Survey of Austria, Vienna, Austria
[6]Eurasia Institute of Earth Sciences, İstanbul Technical University, İstanbul, Turkey
[7]Biostratigraphic Associates (UK) Ltd, Stoke on Trent, UK
[8]Montanuniversitaet Leoben, Leoben, Austria
[9]OMV New Zealand Ltd, Wellington, New Zealand
[10]OMV Exploration & Production GmbH, Vienna, Austria

Received: 04.07.2019 • **Accepted/Published Online:** 04.09.2019 • **Final Version:** 02.01.2020

Abstract: The biostratigraphy and paleoenvironments of the İhsaniye Formation exposed at Karaburun in northwest Turkey is described based upon the study of abundant and well-preserved foraminifera, calcareous nannofossils and palynomorphs. The studied succession is Early Oligocene in age, with calcareous nannofossil zones upper NP21 (Subzone CNO1) to lower NP23 (Subzone CNO3) and planktonic foraminifera zones O1 (~P18) and O2 (~P19) represented, and palynological assemblages suggestive of zones D13 to D14a. Based on these new data, a revised interpretation of the stratigraphic succession is presented. Deposition was controlled by a now inverted normal fault, with deposition of older stratigraphy (upper NP21 to NP22) restricted to the original hanging wall. During NP23, deposition commenced on the footwall, resulting in progressive onlap of an exposed Eocene reefal limestone (Soğucak Formation). Three primary sedimentary facies are present: marls with thin calcareous siltstones, marls with synsedimentary slumps and debris flows, and coarse pebbly sandstones. The coarse pebbly sandstones were deposited in a fan-delta/shoreface paleoenvironment and represent the initial phase of onlap during biozone NP23 onto a rocky shoreline on the footwall side of the fault. The marl-dominated facies represent deposition in outer shelf–upper bathyal environments. The succession demonstrates evidence for a near-end Eocene relative sea-level fall. Changes in the abundance of planktonic foraminifera and the onlap onto the footwall demonstrate maximum subsequent transgression within NP23. This reflects eustasy rather than Paratethyan relative sea-level. No interpretation of sea-water salinity reduction can be made for the sediments deposited during biozone NP23 in the studied sections, although this is noted in coeval sediments in parts of Paratethys (the "Solenovian Event"). Together with the open marine nature of the diverse and abundant fossil assemblages, it is suggested that deposition of the Karaburun section was strongly influenced by a connection to the global ocean, via the Çatalca Gap, as suggested in a recent study.

Key words: Oligocene, Black Sea Basin, Thrace Basin, biostratigraphy, paleoenvironments

1. Introduction

The town of Karaburun is located on the Black Sea coast of Turkey approximately 60 km to the northwest of İstanbul (Figure 1). North of the town is a prominent cape formed by Late Eocene reefal limestones of the Soğucak Formation (Figure 2). To the south and west of the cape, a section can be followed, mostly at beach level, of marls, coarse pebbly sandstones and debris flows, assigned to the İhsaniye Formation (Figures 2–6). The correct stratigraphic order of the facies present requires biostratigraphic control to elucidate because the section is interrupted by a major fault (a now inverted normal fault that had an evidently significant control on deposition). To the south of the major fault is a 70-m thick succession ("Hanging Wall Section"), consisting mostly of marls, but with slumps and debris flows in its upper part (Figure 6). Gentle dips mean that this part of the succession is exposed over a section approximately 1.5 km in length. To the east and north of the fault ("Footwall Section") are pebbly sandstones and marls that onlap the reefal limestones of the Soğucak Formation

* Correspondence: mike.simmons@halliburton.com

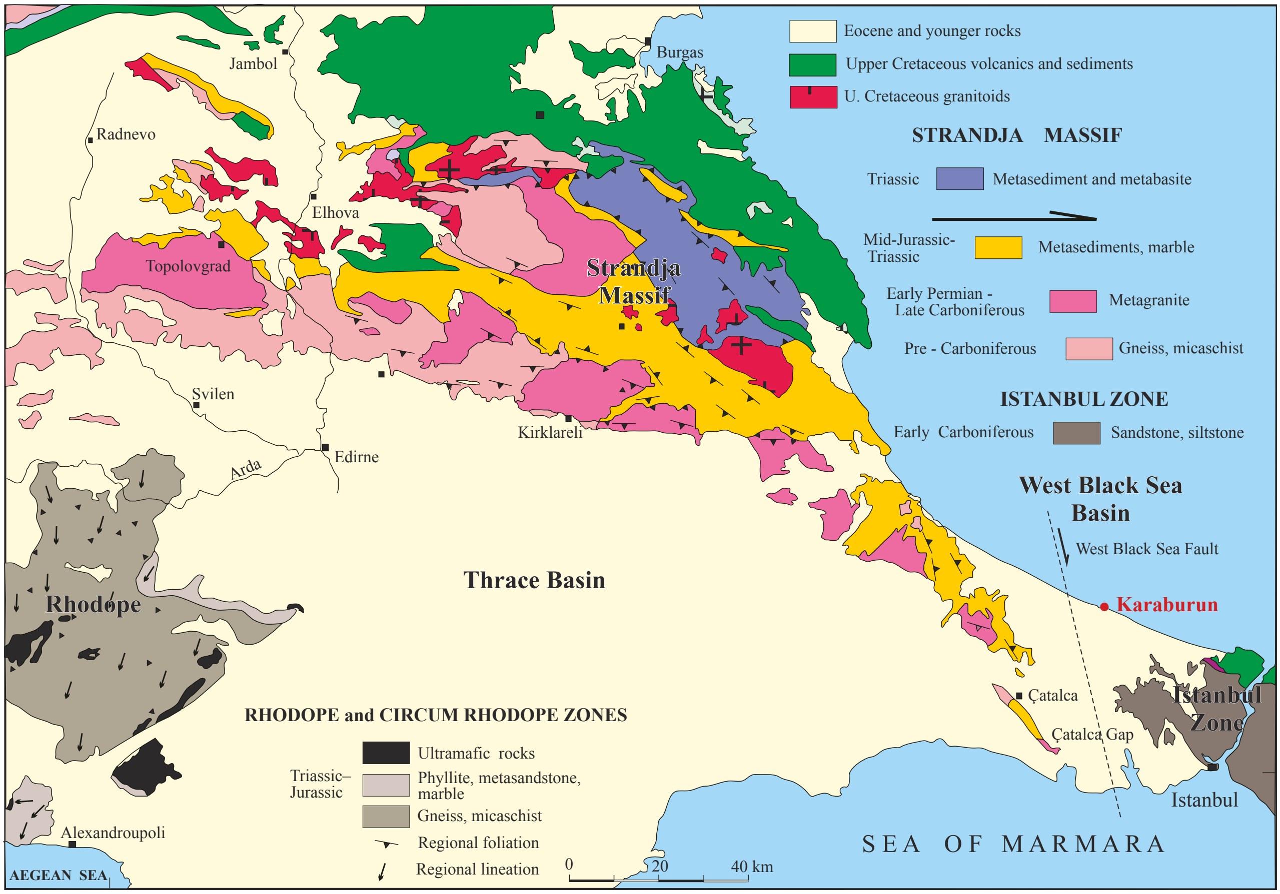

Figure 1. Location of Karaburun in relation to Thrace Basin, Strandja Massif, and Çatalca Gap aligned along West Black Sea Fault. Geological map after Okay et al. (2001).

and are exposed in a series of coves and on the hillside of the cape (Figures 3 and 4). A further transpressional fault is thought to interrupt the succession (Figure 2) but the stratigraphic series can still be followed.

A primary objective of this research has been to use the well-preserved and often abundant and diverse assemblages of calcareous nannoplankton, foraminifera, and palynomorphs to determine the detailed biostratigraphy and age calibration of the İhsaniye Formation. Previous studies have been limited to a few samples, mostly from the lower part of the formation (Sakınç, 1994; Less et al., 2011; Okay et al., 2019). Additionally, the diverse assemblages of microfossils present assist in determining the paleobathymetry and depositional setting of the İhsaniye Formation at this location and the vertical stratigraphic patterns or paleoenvironmental trends.

At the time of deposition, the studied outcrop was located on the margins of Paratethys (Figure 7), the semiisolated seaway formed at the end of the Eocene as a result of orogenic uplift and eustatic sea-level fall (Rögl, 1999; Schultz et al., 2005; Popov et al., 2002, 2010; van der Boon et al., 2018). Therefore, Oligocene deposition in Paratethys reflects a period of dramatic geological change, as apparent in the typical depositional successions observed throughout the region (Ozsvárt et al., 2016), not least around the margins of the Black Sea (Sachsenhofer et al., 2018). Here, in a rock unit often referred to as the Maykop Suite, the succession often becomes clay- and sand-dominated (as opposed to carbonate-dominated as in the underlying Eocene succession) and often contains a moderately high content of organic carbon, making it a key potential source rock within the region (Bazhenova et al., 2003; Sachsenhofer et al., 2017, 2018; Gavrilov et al., 2017). Sandstones within the Maykop Suite succession also have potential as hydrocarbon reservoirs (Tari et al., 2009, 2011; Rees et al., 2018; Simmons et al., 2018; Tari and Simmons, 2018). Consequently, the stratigraphic and paleoenvironmental description of the İhsaniye Formation which is a lateral equivalent of the Maykop Suite enables an improved understanding of the regional depositional framework of Oligocene sediments in Paratethys with an impact for predicting both source rocks (Tulan et al., 2020) and reservoirs (Rees et al., 2018) of this age in the Black Sea depocenter. Note that the İhsaniye Formation

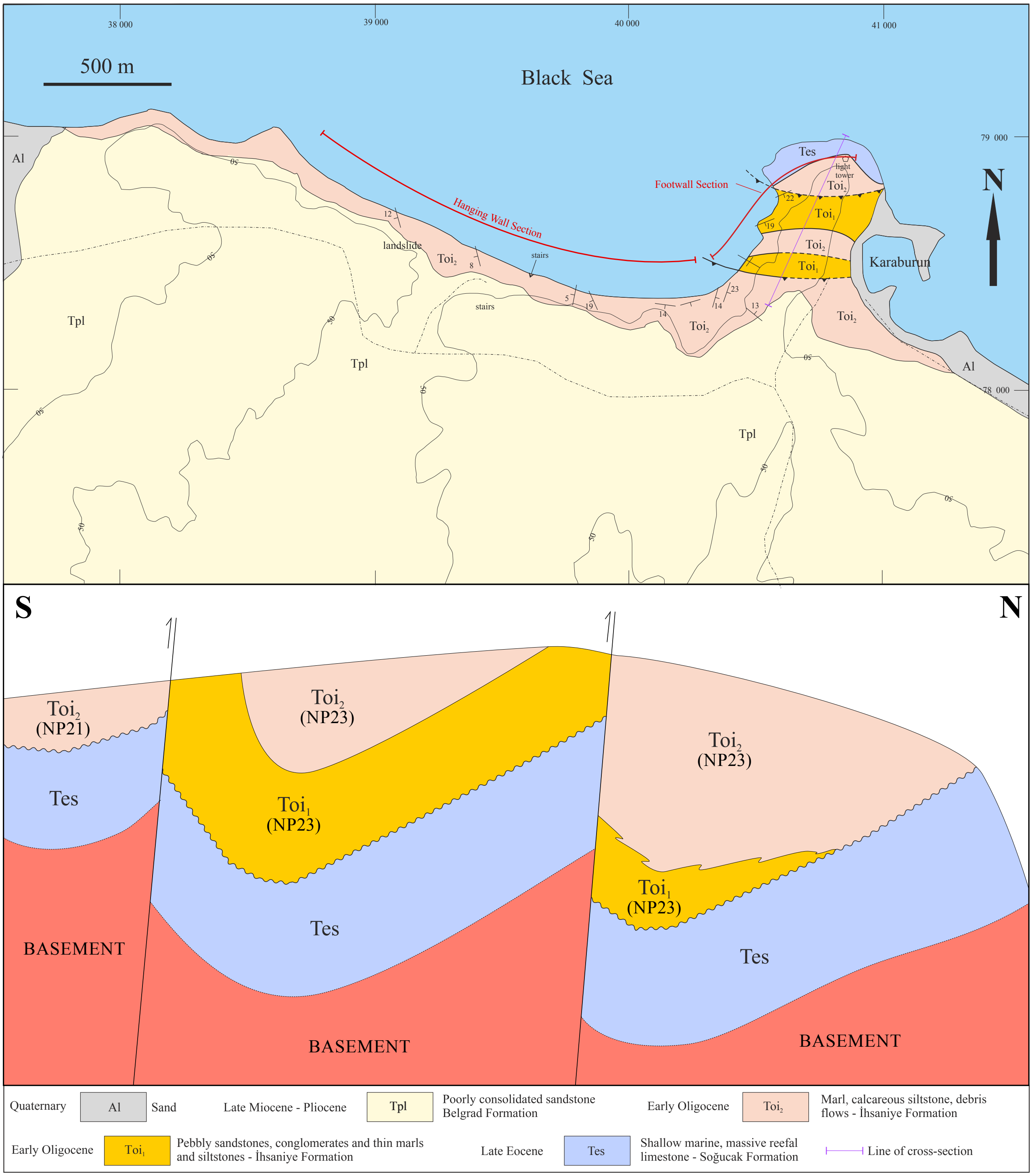

Figure 2. Geological map and cross-section of the Karaburun region showing the location of the studied sections (revised after Okay et al., 2019). Revisions account for the biostratigraphic data reported herein. The fault toward the north of Cape Karaburun is conjectural, but is necessary to explain the stratigraphy present.

at Karaburun is mostly marly (as opposed to purely siliciclastic) and contains a fully open marine diverse fauna with no evidence for restriction and only limited evidence for bottom-water anoxia within its lower part. This might reflect a proximity to a global ocean marine connection to the south through the Thrace Basin, as suggested by Okay et al. (2019). An objective of this study was to investigate additional evidence for and against such a connection.

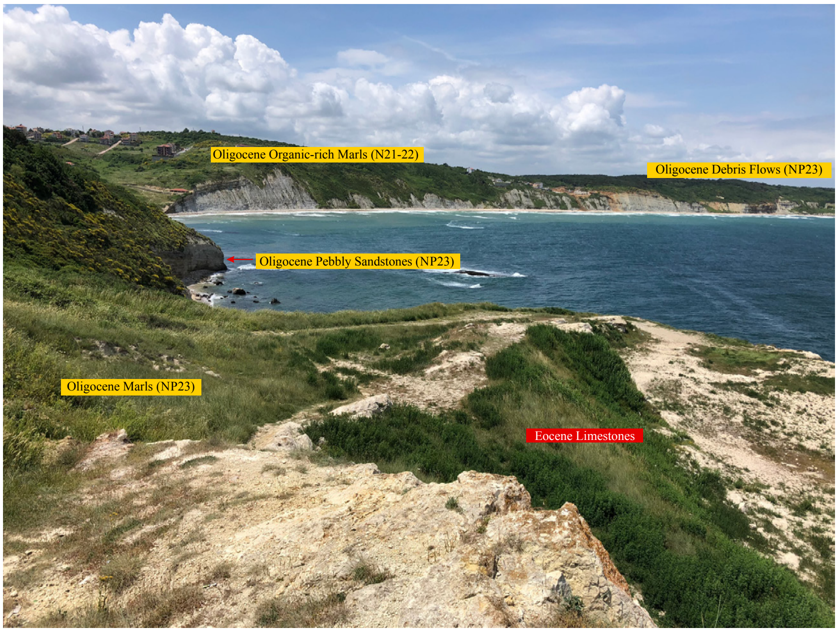

Figure 3. Overview of the studied sections looking south from Cape Karaburun. The Footwall Section is in the foreground with Early Oligocene marls (İhsaniye Formation) onlapping the eroded upper surface of the Soğucak Formation. The Hanging Wall Section is visible in the distance with older Oligocene stratigraphy present as depicted in Figure 6. NP = standard nannoplankton biozone.

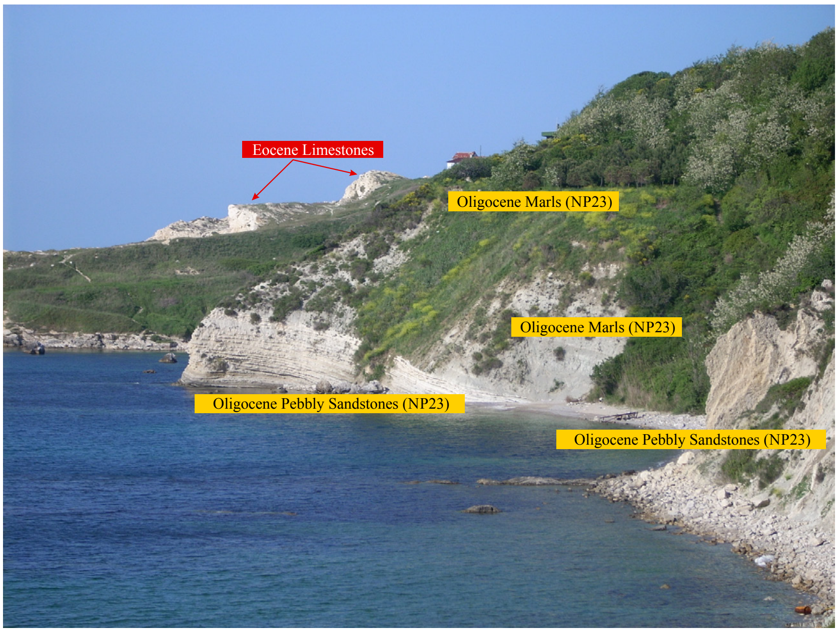

Figure 4. Biostratigraphic data summarised on outcrop photograph of the Footwall Section. NP = standard nannoplankton biozone.

2. Geological setting

The Karaburun region is located near the boundary of two major structural elements: the İstanbul Zone in the east and the Rhodope-Strandja Massif in the west (Figure 1). These elements became juxtaposed in the Late Cretaceous. The İstanbul Zone can be correlated with the Moesian Platform and was displaced southward in the Late Cretaceous along the West Black Sea Fault (Okay et al., 1994). Upper Eocene shallow marine limestones that cover both the Strandja Massif and the İstanbul Zone provide an upper age limit for fault activity (Figure 8). The Late Eocene marine transgression followed an important phase

Figure 5. Biostratigraphic data summarized on outcrop photograph with Footwall Section in foreground and Hanging Wall Section in background beyond the location of the inverted normal fault that controlled deposition of the İhsaniye Formation. NP = standard nannoplankton biozone.

of Late Paleocene–Early Eocene uplift and erosion, related to the collision between the Pontides and the Anatolide-Tauride Block. Shallow marine Eocene limestones, locally with a basal clastic unit, lie unconformably over older units, including Carboniferous sandstones of the İstanbul Zone and metamorphic and plutonic rocks of the Strandja Massif (Varol et al., 2009; Less et al., 2011; Özcan et al., 2020; Okay et al., 2010, 2020).

Karaburun lies on the southern margin of the Western Black Sea Basin that was formed during the Cretaceous. The Strandja Massif separates this basin from the Thrace Basin to the south. The inception and development of the Thrace Basin (Figure 8), a siliciclastic-dominated basin with more than 9 km of sediments within its central part, occurred during the Eocene (Turgut et al., 1991; Görür and Okay, 1996; Siyako and Huvaz, 2007). During the Eocene and Oligocene, the Strandja Massif formed a wide low-relief ridge separating the two basins, as reflected in Late Cretaceous apatite fission-track ages (Cattò et al., 2017). Therefore, although close to the Thrace Basin, the geology of much of the Karaburun succession is quite distinct from the age-equivalent successions deposited in the Thrace Basin (Okay et al., 2019); in general, it has a more open marine character. Comparison with subsurface sections in the western Black Sea is hindered by the lack of published descriptions.

Okay et al. (2019) demonstrated that for parts of Late Eocene and Early Oligocene time, a marine connection existed between the Thrace and Western Black Sea Basins, via the Çatalca Gap west of İstanbul (Figures 1 and 7). This lies along the damage zone of a major Cretaceous West Black Sea strike-slip fault, forming a 15-km wide gateway where carbonate-rich sediments with a maximum thickness of about 350 m were deposited.

3. Regional stratigraphy

Both Thrace and the Karaburun regions have a common shallow marine carbonate unit underlying the Oligocene sequence. This is the Soğucak Formation (Figure 8), age-calibrations by benthic foraminifera demonstrating that it is diachronous within the Middle–Late Eocene, although Priabonian in the Karaburun region (Özcan et al., 2010, 2018; Less et al., 2011; Okay et al., 2019; Yücel et al. 2020). In the Thrace Basin, the Soğucak Formation is succeeded by a relatively thick regressive siliciclastic sequence ranging from Late Eocene to Early Oligocene in age (Figure 8). In the central part of the Thrace Basin, the succession begins with turbidites (Keşan and Ceylan formations) and passes up into pro-delta shales with sandstones (Mezardere Formation) (e.g., Siyako and Huvaz, 2007). Recent work (Gürgey and Batı, 2018) demonstrates that the Mezardere Formation is at least partly Early Oligocene in age and thus age-equivalent to the İhsaniye Formation. These are in turn overlain by continental sandstones and mudstones with lignite horizons (Osmancik and Danişmen formations). Provenance studies indicate a source of clastic material predominantly from the west and southwest from the Rhodope Massif (Cavazza et al., 2013).

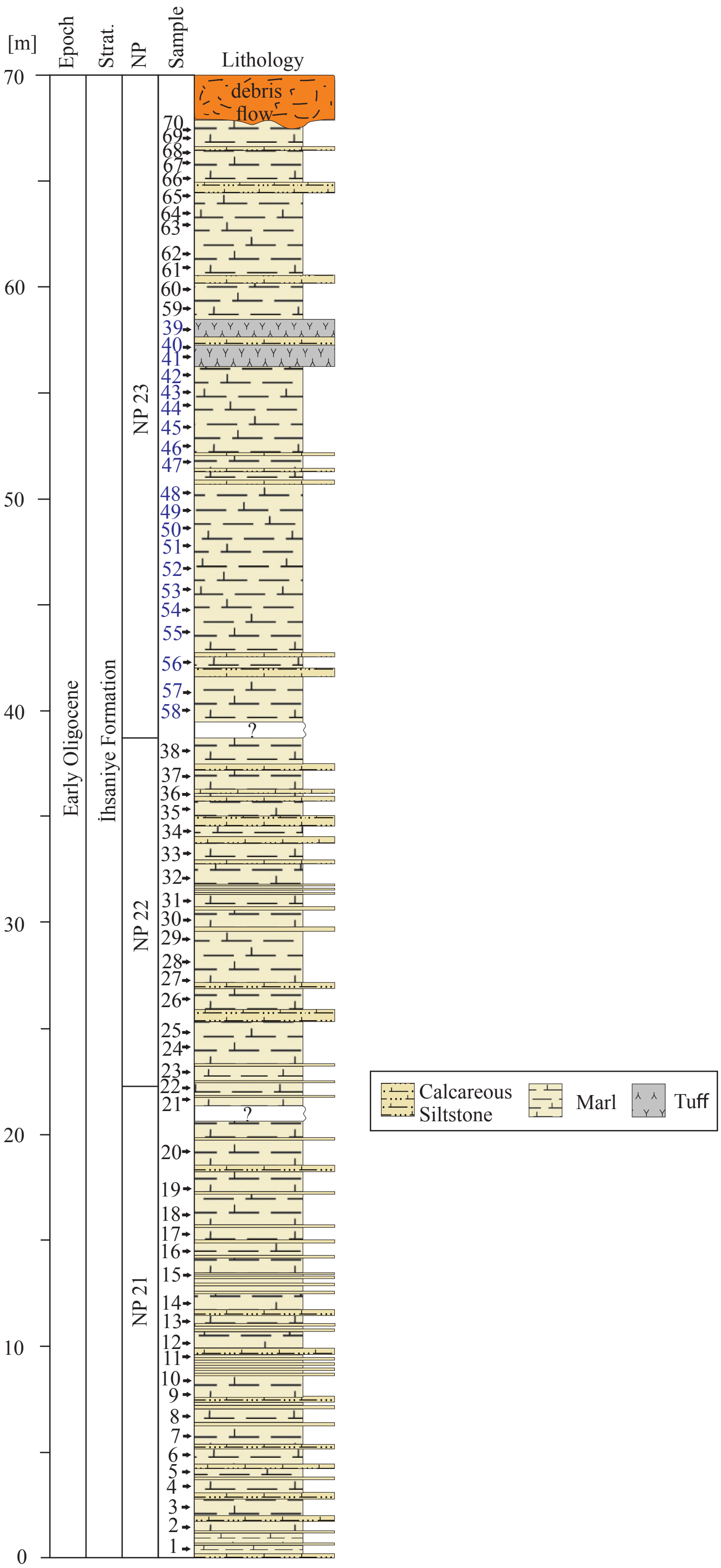

Figure 6. Sedimentary log and sampling points of the İhsaniye Formation within the Hanging Wall Section, Karaburun. NP = standard nannoplankton biozone.

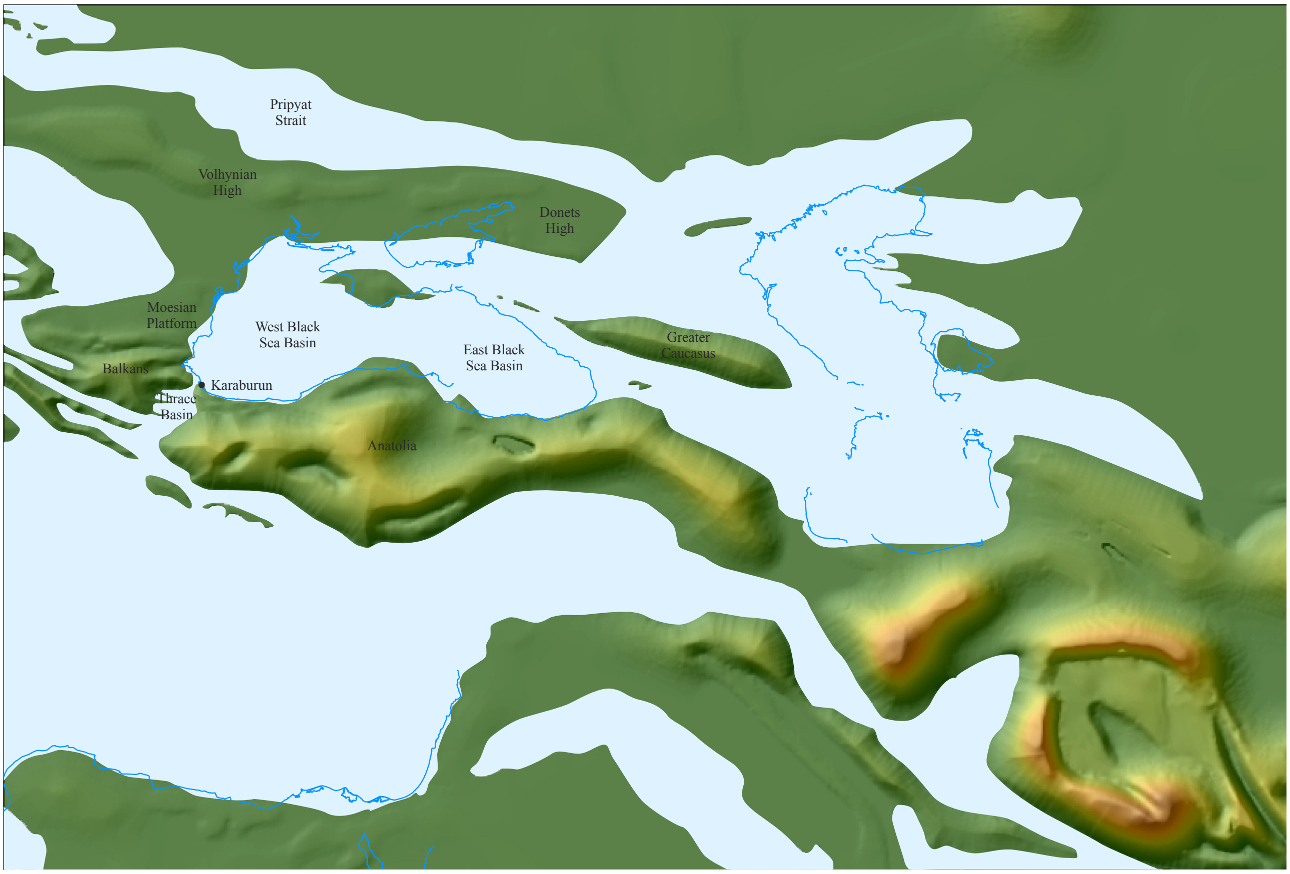

Figure 7. Simplified regional paleogeographic setting of the Early Oligocene of Eastern Paratethys, modified and synthesized after various sources notably Popov et al. (2004).

The general stratigraphic sequence in the Karaburun region also begins with the shallow marine Eocene limestones of the Soğucak Formation; however, in contrast to the succession in the Thrace Basin, these are overlain by a 90-m thick Early Oligocene succession comprising mostly marls/carbonate siltstones (with synsedimentary slumps and debris flows higher in the succession) and coarse pebbly sandstones overlying an erosional unconformity at the top of the Eocene limestone succession. It is this succession that forms the focus of this study.

Within several papers, the Early Oligocene sequence at Karaburun is attributed to the Ceylan Formation, a term used in the Thrace Basin (e.g., Siyako and Huvaz, 2007; Elmas, 2012; Natal'in and Say, 2015). However, the Ceylan Formation in the Thrace Basin consists predominantly of (Eocene) sandstone and shale and is thus an inappropriate term, because the section at Karaburun is much more calcareous and fine-grained (i.e. is mostly composed of marls). The Geological Survey of Turkey (e.g., Yurtsever and Çağlayan, 2002; Gedik et al., 2014) used the term İhsaniye Formation for the sequence above the Soğucak Formation in the Karaburun region, and that practice is followed herein (see also Okay et al., 2019). This may be a synonym for the term Karaburun Formation as used by Lom et al. (2016) who described that unit as "Upper Eocene–Lower Miocene" and overlying the Soğucak Formation in the Karaburun region. Their brief description matches some aspects of the İhsaniye Formation but might include younger formations.

According to the information in the "Lithostratigraphic Guide for the Thrace Region" (Siyako 2006), the Ceylan Formation was first described and defined as the "Ceylan Shale" by Ünal (1967)[1] from Ceylan-1 well in northern Thrace basin. Ünal (1967) is a private Turkish Petroleum internal report not available publicly. The log of the Ceylan-1 well is also not published. Siyako (2006) states that in Ceylan-1 well, the Ceylan Formation consists of 28 m of shale. In the "Lithostratigraphic Guide for the Thrace

[1] Ünal OT (1967). The geology of Thrace and its petroleum potential. TPAO Arama Grubu Arşivi, unpublished technical report, 391 (in Turkish).

Region" the type section of the Ceylan Formation is said to be on the Gelibolu Peninsula between the village of Tayfur and the Tayfur reservoir. The Tayfur section, as described in d'Atri et al. (2012) under the name of Tayfur Formation, consists of siltstone and shale with sandstone beds and with one large slumped tuff horizon (section 2 in Figure 2). The Lithostratigraphic Guide for the Thrace Region also gives the road between Gölcük and Şarköy as a reference section (Siyako 2006). The Gölcük–Şarköy section, described in Okay et al. (2010) consists of sandstone and shale with several mass flow horizons (olistostromes). In contrast, the İhsaniye Formation, defined and mapped by Geological Survey (MTA) geologists (Yurtsever & Çaglayan, 2002; Gedik et al., 2014) consists predominantly of marl (90% of the formation) with minor limestone and tuff. Thus, it is lithologically quite distinct from the Ceylan Formation in its type and reference sections, and has a distinct distribution in the Çatalca Gap.

As noted by a number of authors, the succession above the Soğucak Formation at Karaburun is unlikely to be as old as Late Eocene, although the oldest İhsaniye Formation in contact with the Soğucak Formation is not exposed. Our data and that of Sakınç (1994), Less et al. (2011) and Okay et al. (2019) suggest an Early Oligocene age at Karaburun, although the İhsaniye Formation might be latest Eocene within the Çatalca Gap (Okay et al., 2019) (Figure 8).

Tuffs within the İhsaniye Formation, which are rare at Karaburun, but more common to the south and west (Okay et al., 2019), are most likely the products of volcanic activity in the western part of the Thrace Basin and Rhodope Massif, where Lower Oligocene magmatic rocks are widespread (Eleftheriadis and Lippold, 1984; Ercan et al., 1988).

The İhsaniye Formation is unconformably overlain by continental mudstones and sandstones with lignite horizons of Late Oligocene–Early Miocene age (Ağaçlı Formation: Nakoman, 1968; Gedik et al., 2014; Suc et al., 2015) or (as in the case at Karaburun) by Late Miocene–Pliocene poorly consolidated sandstones (Belgrad Formation: Yurtsever and Çağlayan, 2002; Gedik et al., 2014).

Southwards, close to the town of Çatalca, İhsaniye Formation marls are replaced by mudstones and shales. Close to the Çatalca ridge forming the partial barrier between the Thrace Basin and the Western Black Sea Basin, lagoonal pebbly limestones and pebbly sandstones occur, termed the Pınarhisar Formation (Figure 8). This facies passes up into paper shales with fossil fish.

4. Previous work

The basic geology of the Karaburun region was first described in detail by Erentöz (1949) and Akartuna (1953). Geological maps of the region were published by Yurtsever and Çağlayan (2002), Duman et al. (2004) and Gedik et al. (2014). Previous studies of the İhsaniye Formation at Karaburun include those of Oktay et al. (1992), Sakınç (1994), Natal'in and Say (2015), and Okay et al. (2019). Less et al. (2011) make minor mention of this unit (which they term Ceylan Formation) within their study that concentrated on the Soğucak Formation.

Quite different interpretations of the stratigraphic succession within the İhsaniye Formation at Karaburun have been given by previous workers. Sakınç (1994) and Okay et al. (2019) placed the pebbly sandstones at the base of the succession (i.e. directly overlying the Soğucak Formation limestones); with the succession then passing up into marls and eventually debris flows. The description by Natal'in and Say (2015) is very different. They place the distinctive beds of pebbly sandstones above the marls of the İhsaniye Formation (their Ceylan Formation) and regard the top of the Soğucak Formation as a fault, while we and others (Sakınç, 1994; Less et al., 2011; Okay et al., 2019) consider it as an unconformity. Our work demonstrates that without the benefit of precise biostratigraphic control and an understanding of the importance of fault-controlled deposition, no previous interpretation of the stratigraphic succession is correct. We now recognize a more complex pattern in which deposition of earliest Oligocene marls is initially restricted to the hanging wall of a now inverted major normal fault, with deposition transgressing the footwall (and topographically highest Eocene reef of the Soğucak Formation) later during the Early Oligocene, initially with pebbly sandstone deposition and subsequently with marl deposition (Figure 9).

5. Materials and methods

The collection of samples for study around Karaburun followed two different strategies depending on location. The approximately 70-m dominantly marly section exposed along the beach to the west of the town and of the major fault (the Hanging Wall Section) was logged in terms of primary lithology changes and key sedimentary features and systematically sampled, with sample spacing approximating to every meter (Figure 6). Here, we report on the biostratigraphic analyses employed on these samples (foraminifera, calcareous nannofossils, and palynomorphs). Detailed organic geochemistry and strontium isotope analysis are reported elsewhere (Tulan et al., in press.).

To the north and east of the fault, closer to the cape (the Footwall Section), spot sampling took place with 30 samples collected from marls and marls within the pebbly sandstone that onlap the Soğucak Formation. These were analyzed for foraminifera and calcareous nannofossils.

In total, 100 samples were prepared for foraminiferal analysis using the standard methodology described by

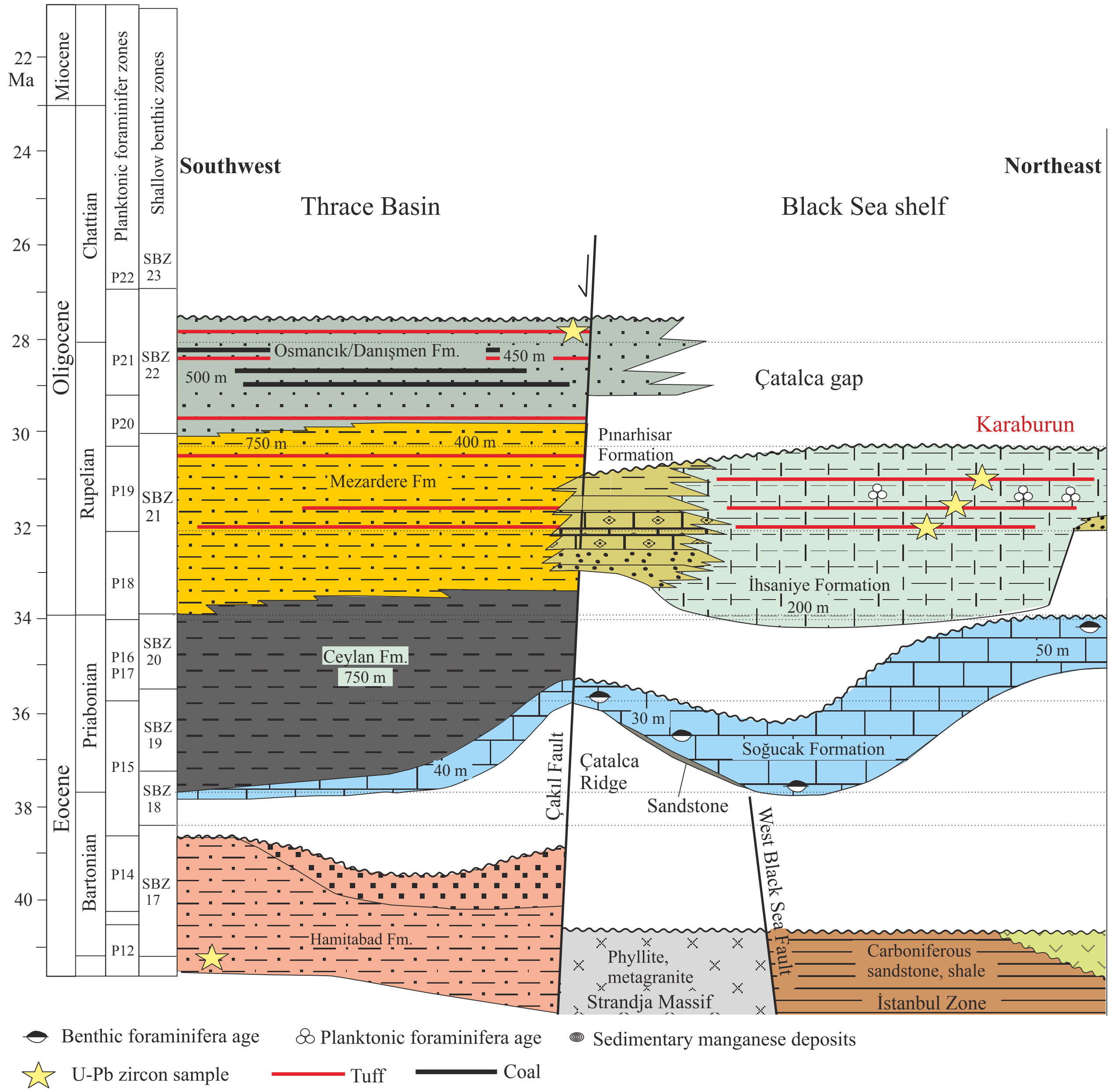

Figure 8. Regional stratigraphy summary of the Late Eocene–Oligocene succession in northwest Turkey (revised after Okay et al., 2019). The age of the Mezardere Formation is revised after Gürgey and Batı (2018). The age of the oldest İhsaniye Formation in the region of the Çatalca Gap is based on a reinterpretation of the foraminiferal data in Okay et al. (2019); for example, some taxa recorded by these authors (particularly *Tenuitella gemma*) cannot be older than very latest Eocene; 300 Ka below base Oligocene (refer to text and http://orca.cf.ac.uk/15234/). The age of the stratigraphy around Karaburun is revised after the interpretations here; note the fault control on deposition as discussed in the text. Despite these revisions, uncertainty remains, particularly in terms of age calibration of the Thrace Basin stratigraphy.

Armstrong and Brasier (2005). To summarize, dissolution in a 10% solution of hydrogen peroxide was undertaken, and the residues dried and then concentrated using a nest of sieves. Foraminifera (and ostracoda and other miscellaneous microfossils) were then transferred to slides for examination with a binocular microscope. 15 additional samples of indurated rock (top Soğucak Formation and cemented calcareous sandstones within the İhsaniye Formation) were studied in thin section.

One hundred samples were investigated semi-quantitatively for calcareous nannofossils. Smear slides were prepared following standard procedures described by Perch-Nielsen (1985) and examined under a light microscope (Leica DMLP) using cross and parallel nicols with 1000× magnification.

Eighteen samples were prepared for palynological analysis using the standard methods described by Armstrong and Brasier (2005). Approximately 30 g of cleaned and crushed sample was used for processing. Standard HCl (20%) and HF (40%) chemical treatments were sequentially used to dissolve the carbonate and silicate content of the samples. Multiple resieving over 10-µm mesh cloth, including rewarming in 20% HCl to remove silico-fluoride precipitates, was performed. The sample was then assessed to establish further processing requirements (oxidation) to concentrate the palynomorphs present (a split of the unoxidized kerogen was taken at this time). Oxidation involved cold bathing in concentrated nitric acid (70%) for between 2 and 5 min, followed by further sieving and neutralization with water. Further microscopic examination determined the amount of ultrasonic treatment (between 5 and 15 s), which helped to concentrate the palynomorphs further. Both unoxidized and oxidized kerogen residues were separately mounted onto a labelled glass slide and permanently glued using Norland optical adhesive No. 63.

6. Outcrop description

6.1. Soğucak Formation

The fossiliferous limestones of the Soğucak Formation at Karaburun are described in detail by Less et al. (2011). A succession approximately 60-m thick is well exposed within old quarries on Cape Karaburun to the north of Karaburun town where the limestones are massive to thickly bedded, with some beds consisting of coral bioherms. The occurrence of larger foraminifera (*Heterostegina gracilis*, *Spiroclypeus carpathicus*, *Asterocyclina stella*) enabled Less et al. (2011), Okay et al. (2019), and Yücel et al. (2020) to assign the succession to Standard Larger Benthic Foraminifera Biozone (SBZ) 20 which suggests a latest Eocene (late Priabonian) age (Serra-Kiel et al., 1998) (Figure 10). In our material from the uppermost Soğucak Formation at Cape Karaburun, we recorded *Orbitolites* sp. (possibly *Orbitolites complanatus*), *Linderina* sp., possible *Praebullalveolina afyonica*, and *Idalina grelaudae*, along with rare orthophragmid foraminifera and globigerine planktonic foraminifera (Figure 11). While the occurrence of the named species is compatible with a Priabonian age, *Orbitolites* is typically associated with biozones older than SBZ20 (Jones and Racey, 1994; Serra-Kiel et al., 1998, 2016), although was previously recorded (without illustration) by Less et al. (2011) from the Soğucak Formation at Karaburun. The foraminiferal assemblage include both back-reef, lagoonal, components (large miliolids, alveolinids, *Orbitolites*) and fauna more typical of fore-reef communities (orthophragmids and planktonic foraminifera) alongside reef-forming corals and coralline red algae, suggesting strong syndepositional mixing.

The base of the Soğucak Formation is not exposed but these limestones probably lie over Late Cretaceous volcanic rocks that crop out further east along the coast (Okay et al., 2019).

The upper surface of the limestones has a markedly erosional profile, with marls of the overlying İhsaniye Formation infilling erosional depressions and pockets (Figure 12a). In the upper part of the limestone succession, a fissure (neptunian dyke) is infilled with material from the overlying İhsaniye Formation indicating that the limestones of the Soğucak Formation were lithified before deposition of the İhsaniye Formation and is a further indication of an unconformable contact between the two units (Okay et al., 2019; Yücel et al., in press). This boundary is a very abrupt contact, and a hardground is indicated by the presence of brownish iron oxide-rich concretion on the uppermost surface of the Soğucak Formation. Blocks of the Soğucak Formation are found reworked in the overlying İhsaniye Formation.

6.2. İhsaniye Formation

In places, a thin (1 cm) poorly-sorted sandstone with volcanic clasts plasters the upper surface of the Soğucak limestones and is a poorly preserved deposit representing initial İhsaniye Formation deposition. In thin-section angular quartz; lithics, chlorite, miliolid foraminifera, and fragments of calcareous red algae are present.

In the Footwall Section there are two parts to the İhsaniye Formation (Figure 4):

(i) The lowest part comprises approximately 15 m of medium bedded, mixed pebbly calcareous sandstones (or “gravelstones”), siltstones, and calcarenites with rare thin (<1 m) marl interbeds (Figure 12b). Overall this part of the succession fines up so that the coarsest facies lie in the lower approximately 5 m, where pebbly sandstones/gravelstones predominate. Higher in the section, coarse sands with only occasional pebbles occur. Grading (both normal and reversed) (Figure 12c) provides distinct bedding, but there are few other sedimentary structures other than rare large (meter-scale) cross-bedding. Imbrication and trace fossils are absent. The clasts within the sandstones are mainly rounded, black, gray, and dark-green basaltic andesite and andesite reworked from the Late Cretaceous succession with minor limestone reworked from the Soğucak Formation. The volcanic clasts range in size from medium sand up to 30 cm across; and in a few beds, the clasts are densely packed such that the deposit might be termed a matrix-supported conglomerate. Soğucak Formation limestone clasts are less common but reach 1 m in size. The sandstones consist of carbonate and lithic (volcanic and volcaniclastic) grains with an abundance of bioclasts

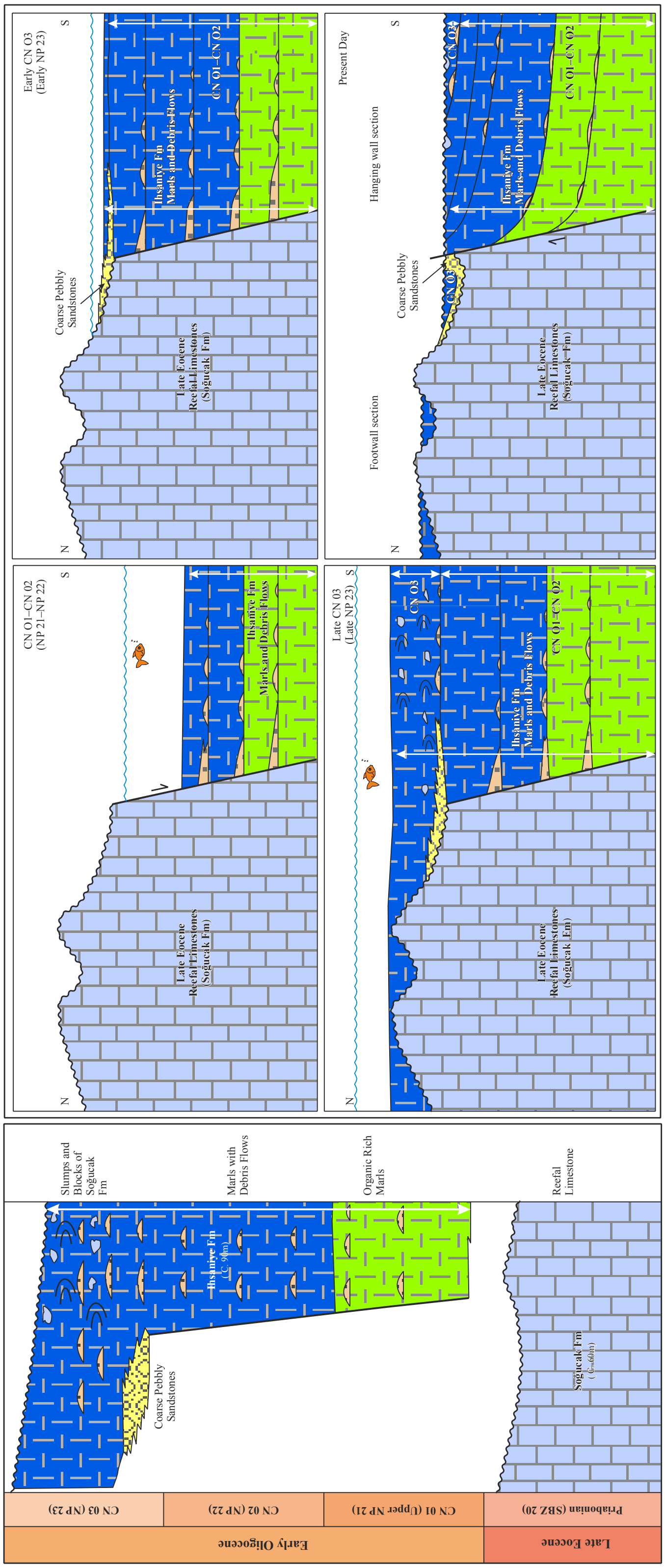

Figure 9. Summary of the stratigraphy and stratigraphic evolution of İhsaniye Formation deposition at Karaburun during the Early Oligocene based on the new biostratigraphic data reported herein.

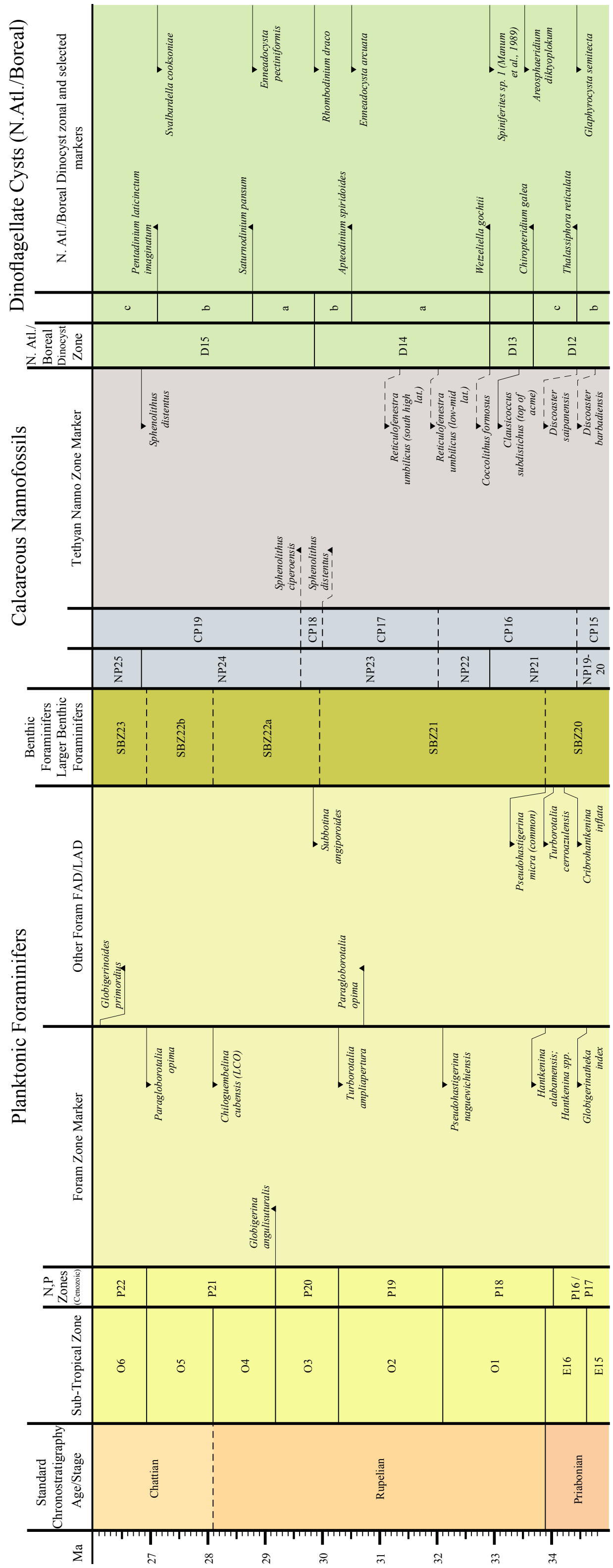

Figure 10. Late Eocene–Oligocene foraminiferal, calcareous nannofossil, and dinocyst biozones and bioevents (in part after Vanderberghe et al., 2012 and created using Timescale Creator Pro and the datapacks therein).

including the larger foraminifera *Nummulites* (*Nummulites vascus* and *Nummulites bouillei* - Sakınç, 1994; Less et al., 2011 and our own observations). Interpretation of the precise depositional setting of this sedimentary package requires further detailed sedimentological studies, but the facies present are reminiscent of fan-delta and shoreface deposition (Wescott and Ethridge, 1990; Colmenero et al., 1988; Marzo and Anadón, 1988; Rees et al., 2017) on a steep rocky shoreline - slope (Nemec, 1990; Colella, 1988; Sheppard, 2006). Presumably, further faults depositionally proximal to the Karaburun location exposed Cretaceous volcanics that were eroded and transported into this facies. Overall, this represents a transgressive deposit grading up into the offshore marls of the overlying facies.

(ii) The pebbly sandstones quickly pass up into an approximately 30 m succession of gray marls with thin (typically approximately 5 cm) calcareous siltstone interbeds (Figure 4), similar to the succession observed on the hanging wall side of the fault. Although disturbed by a likely transpressional fault, the geometry of the succession clearly demonstrates that these marls onlap against the eroded surface of the Soğucak Formation as exposed in the high ground around Cape Karaburun (Figure 3).

On the hanging wall side of the fault there are also two parts to the İhsaniye Formation (Figure 6):

(i) Approximately 40 m of marls (65%) and carbonate-rich siltstone or fine sandstone (30–35%) with minor debris flow horizons containing mainly blocks of the Soğucak Formation. The marls weather to a light gray color but can be dark gray when freshly exposed (Figure 12d). The siltstone and sandstone consist principally of carbonate grains with an admixture of volcanic clasts. Scoured bases, parallel lamination, and fining-up profiles are typical of the sandstone beds (Figure 12e).

(iii) In the remaining 30+ m of the section, debris flows and synsedimentary slumps and folding (Figure 12f) become increasingly common. Debris flows have notable erosional bases forming scours, and beds 5-m thick are amalgamated such that much of the upper part of the section is mostly debris flows with minor marl horizons. Clasts within the debris flows include large (>1 m) angular clasts of Soğucak Formation and of volcanic lithologies reworked from the underlying Late Cretaceous succession.

7. Biostratigraphy

7.1. Calcareous nannoplankton

For all samples, except 39, 40, and 41 from the Hanging Wall Section which might be tuffs, nannofossil recovery was excellent, with a well-preserved and diverse flora (Figure 13). This enabled the standard biozonation of Martini (1971) to be utilized as modified by Agnini et al. (2014) and Okada and Bukry (1980) (Figure 10).

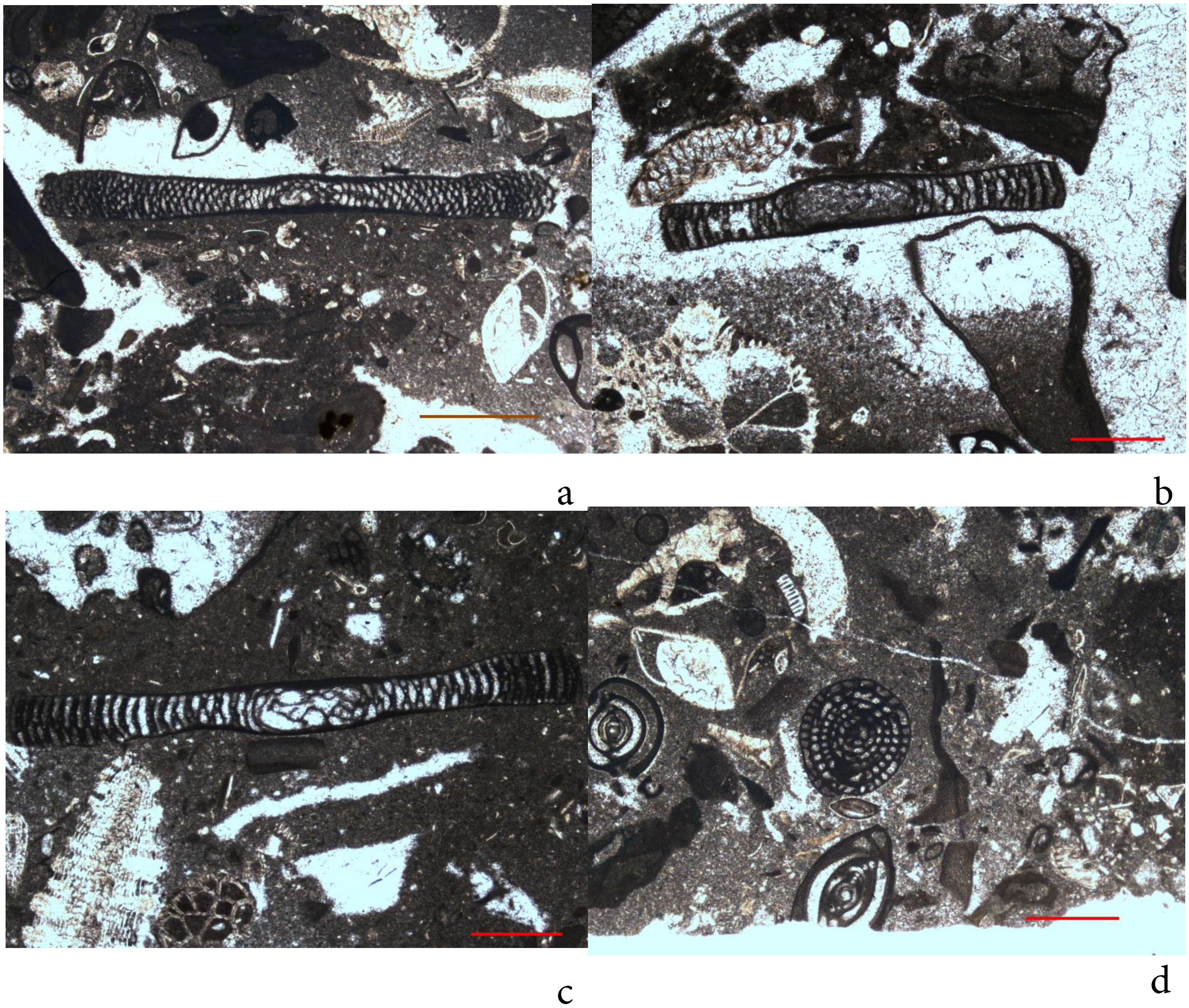

Figure 11. Larger foraminifera present in the uppermost Soğucak Formation exposed on Cape Karaburun. Scale bar (a) 1000 µm, (b)–(d) 500 µm. (a) – (c) *Orbitolites* sp. (possibly *Orbitolites complanatus),* (d) *Praebullalveolina afyonica*? and *Idalina grelaudae*.

The following three nannofossil biozones could be recognized in the studied material (Figure 14):

- Samples 1 to 22 (Hanging Wall Section): Biozone NP21 (CNO1 Subzone)
- Samples 23 to 38 (Hanging Wall Section): Biozone NP22 (CNO2)
- Samples 58 to 70 (Hanging Wall Section) and all samples from the Footwall section of the İhsaniye Formation: Biozone NP23 (CNO3 Subzone)

7.1.1. Biozone NP21 (CNO1 Subzone)

This zone is defined as the interval between the last (youngest) occurrence (LO) of *Discoaster saipanensis* at its base and the LO of *Coccolithus formosus* at its top. Based on the absence of *D. saipanensis* and *Discoaster barbadiensis* and the presence of *C. formosus* in samples 1 to 22, this part of the section can be assigned into biozone NP21. This zone was recently subdivided by Agnini et al. (2014) into CNE 21 (*Helicosphaera compacta* Partial Range Zone) and CNO1 (*Ericsonia formosa*/ *Clausiococcus subdistichus* Concurrent Range Zone). CNE21 corresponds with the lower (Late Eocene) part of NP21 and the lower Subzone CP16a (Okada and Bukry, 1980), whereas CNO1 corresponds with the upper (Early Oligocene) part of NP21. A significant increase in the abundance of *Clausiococcus subdistichus* defines the base of CNO1. Samples 1 to 22 from the Hanging Wall Section contain high percentages of *C. subdistichus* and can thus be attributed to Subzone CNO1, the Early Oligocene part of NP21.

All samples from this zone contain abundant, well-preserved nannoplankton assemblages dominated

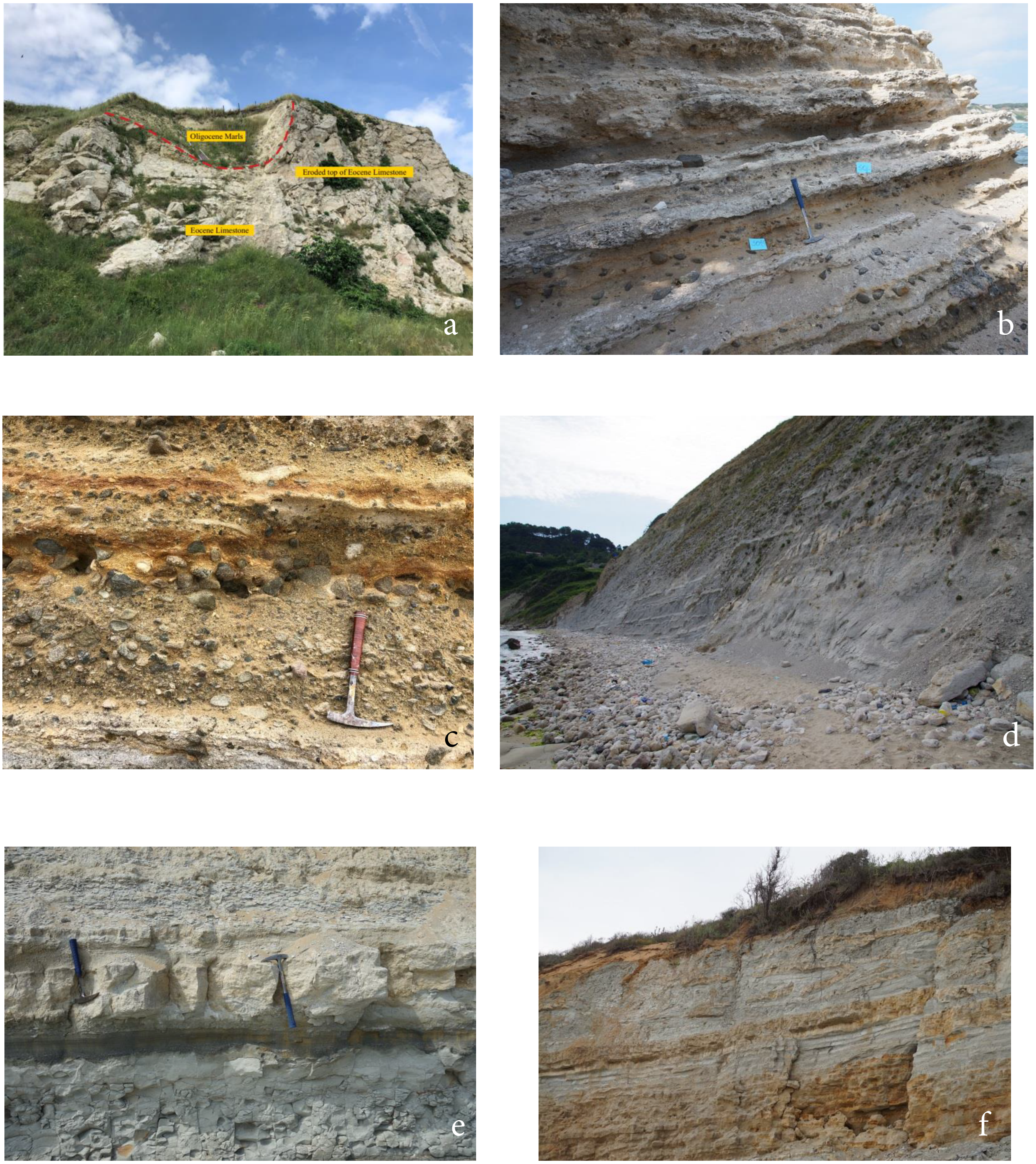

Figure 12. Outcrops photographs from the Karaburun sections. (a) Erosional depression within the top Soğucak Formation infilled with Early Oligocene marls of the İhsaniye Formation, northern Cape Karaburun corresponding to section 1590 in Okay et al. (2019); (b) Pebbly sandstone facies of the İhsaniye Formation, Footwall Section; (c) Possible reverse grading within the pebbly sandstone facies; (d) Marl dominated part of the İhsaniye Formation, Hanging Wall Section. This is the oldest part of the İhsaniye Formation at Karaburun assignable to calcareous nannoplankton zone upper NP21 and planktonic foraminiferal biozone O1. Organic carbon content is relatively rich; (e) Erosively based calcareous sandstone within İhsaniye Formation, Hanging Wall Section; (f) Synsedimentary slumping and folding within the upper part of the İhsaniye Formation, Hanging Wall Section.

by *Cyclicargolithus floridanus* and *Reticulofenestra minuta*. Occurring regularly are *Blackites tenuis*, *C. formosus*, *Coccolithus pelagicus*, *Dictycococcites bisectus*, *Dictycococcites hesslandi*, *Pontosphaera multipora*, *Zygrhablithus bijugatus*. Reticulofenestrids are present with regular occurrences of *Reticulofenestra dictyoda*, *Reticulofenestra hillae*, *Reticulofenestra lockeri*, and *Reticulofenestra umbilicus*. The genus *Helicosphaera* is represented by *Helicosphaera bramlettei*, *Helicosphaera compacta*, *Helicosphaera euphratis*, and *Helicosphaera reticulata*. Rare discoasters are present including *Discoaster deflandrei*, *Discoaster tanii*, *Discoaster nodifer*, and *Discoaster ornatus*. Sphenoliths include regular *Sphenolithus moriformis*, *Sphenolithus predistentus*, and rare *Sphenolithus tribulosus* (First (oldest) occurrence (FO) in NP21). Minor components of the nannofossil assemblage include *Coccolithus eopelagicus*, *Holodiscolithus macroporus*, *Lanternithus minutus*, *Pontosphaera minuta*, and *Pontosphaera pygmaea*.

7.1.2. Biozone NP22 (CNO2)

This zone is defined as the interval between the LO of *C. formosus* at its base and the LO of *R. umbilicus* at its top. Based on the absence of *C. formosus* and the presence of *R. umbilicus* in samples 23 to 38 from the Hanging Wall Section, this part of the section can be assigned to biozone NP22, which correlates to Zone CNO2 of Agnini et al. (2014) and Zone CP16c of Okada and Bukry (1980). The FO of *Helicosphaera recta* is observed in sample 34. This large size helicolith with two large openings in the central area has its FO within NP22.

Assemblages from this zone are very similar to those of NP21 with the dominance of *R. minuta* and *C. floridanus*. The following taxa occur regularly: *B. tenuis*, *C. pelagicus*, *C. subdistichus*, *D. bisectus*, *D. hesslandi*, helicoliths (*H. bramlettei*, *H. compacta*, *and H. euphratis*), *P. multipora*, *R. dictyoda*, *R. hillae*, *R. lockeri*, *S. moriformis*, and *Z. bijugatus*. *Isthmolithus recurvus* which has a LO within NP22, was observed in samples 25 and 31. Discoasters are less common than in Zone NP21, but the same species are present.

7.1.3. Biozone NP23 (CNO3 Subzone)

This zone is defined as the interval between the LO of *R. umbilicus* at its base and the FO of *Sphenolithus ciperoensis* at its top. Based on the absence of both these zonal markers and an abundance of *C. floridanus*, samples 58 to 70 in the Hanging Wall Section and all samples of the İhsaniye Formation from the footwall section can be attributed to biozone NP23. This zone was subdivided into CNO3 (*Dictyococcites bisectus* Partial Range Zone) and CNO4 (*Sphenolithus distentus*/*Sphenolithus predistentus* Concurrent Range Zone) by Agnini et al. (2014). The boundary between them is marked by the FO of *Sphenolithus distentus*. This taxon does not occur in any of the studied samples; therefore, this part of the section is assigned to the lower part NP23, Subzone CNO3.

Most samples contain abundant, well-preserved calcareous nannoplankton assemblages dominated by *C. floridanus* and *R. minuta*. The following taxa occur regularly: *B. tenuis*, *C. pelagicus*, *D. bisectus*, *D. hesslandi*, *Lanternithus minutus*, *P. multipora*, *S. moriformis*, *S. predistentus*, and *Z. bijugatus*. Discoasters are very rare, but are presented by the same species that occur lower within the section. Helicoliths are present including *H. bramlettei*, *H. compacta, H. euphratis* and *H. recta*. Of note is the presence of *Helicosphaera obliqua* and *H. perch-nielseniae*, which have their FO within NP23.

7.2. Foraminifera

For all but three (?tuffaceous) samples, microfossil recovery and preservation was exceptionally good (Figure 15). In many cases samples were significantly overpicked (i.e. many more than 301 specimens were extracted) simply because the washed residues were so rich in microfossils. Diversity of the assemblages present is exceptional with more than 360 individual taxa recorded.

The vast majority of samples contain abundant planktonic foraminifera comprising between 24% and 85% of the total foraminiferal assemblage, with an average value of approximately 52% (Figure 14). The planktonic foraminifera exhibited a distinct Oligocene aspect, with the assemblages being overwhelmingly dominated by non-keeled "globigerinid" forms typical of that period. The assemblages present allowed the standard planktonic foraminiferal biozonation of Wade et al. (2011) to be utilized (Figures 10 and 14).

The following two planktonic foraminiferal biozones could be recognized within the Hanging Wall Section:

- samples 1 to 49: Biozone O1
- samples 48 to 70: Biozone O2

Note that sample numbering does not follow strict numeric order (Figures 6 and 14). For example, sample 48 lies above sample 49.

Footwall section samples lacked taxa that permit assignment to a specific biozone, but are of Early Oligocene aspect (see subsequent discussion). Previous workers have identified the larger foraminifera *N. vascus* and *N. bouillei* with the pebbly sandstone facies (Sakınç, 1994; Less et al., 2011) indicating that these sediments can be assigned to SBZ 21/22 of Cahuzac and Poignant (1997), which, in turn, indicates an Early Oligocene age (Figure 10). We recognized *N. bouillei* in our samples from the Footwall Section.

7.2.1. Biozone O1

Biozone O1 is defined as the interval between the LO of *Hantkenina alabamensis* at its base and the LO of *Pseudohastigerina naguewichiensis* at its top (Wade et al., 2011). Based on the absence of *H. alabamensis* and other

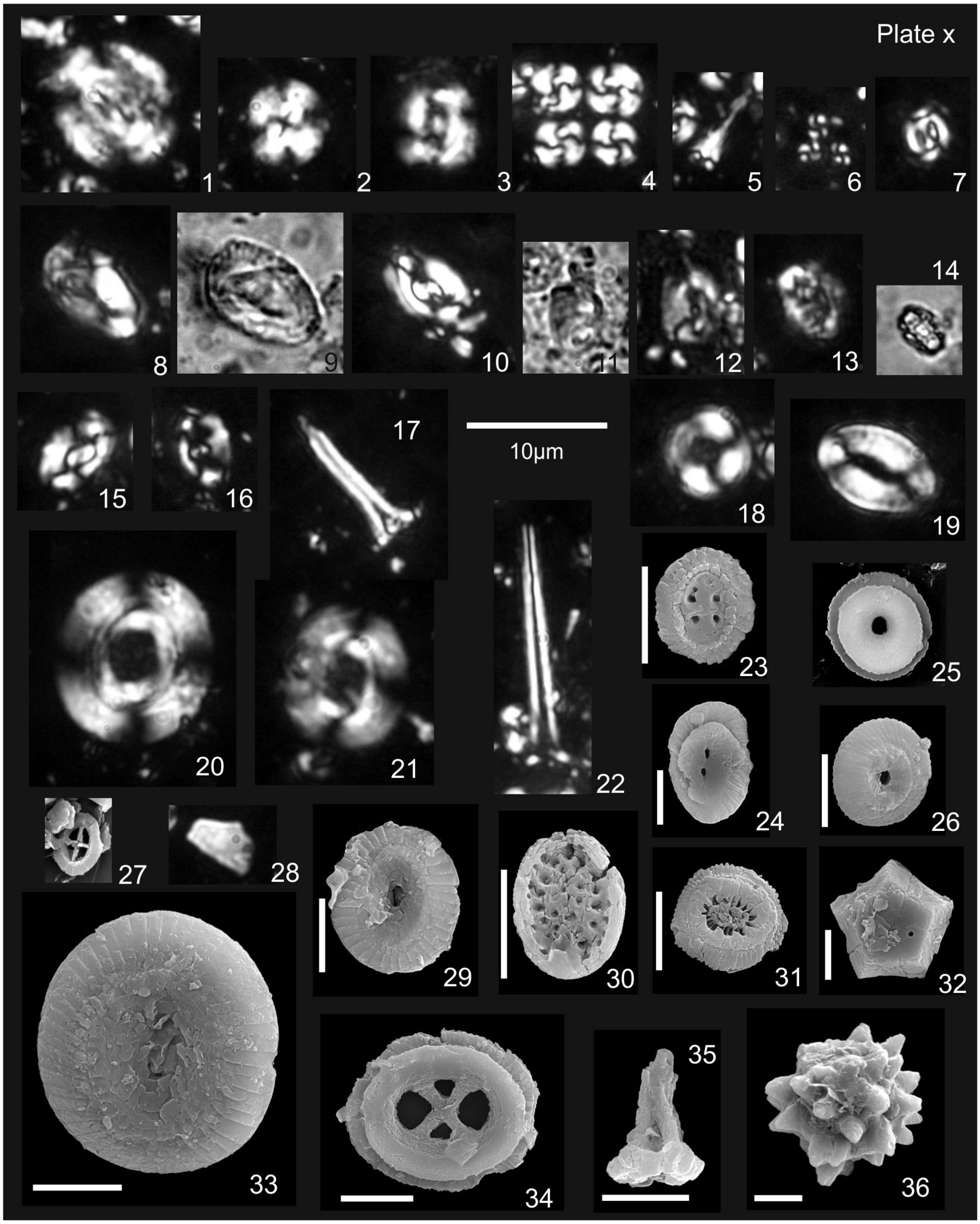

Figure 13. Key calcareous nannofossils from the İhsaniye Formation, Karaburun (10μm scale bar for Light Microscope figures; 5μm for SEM figures.) **1:** *Dictyococcites bisectus* (Hay et al. 1966) Bukry and Percival 1971; Sample 49. **2:** *Dictyococcites hesslandii* Haq 1971; Sample 49. **3:** *Reticulofenestra lockeri* Müller, 1970; Sample 9. **4:** *Cyclicargolithus floridanus* (Roth and Hay, *in* Hay *et al.*, 1967) Bukry, 1971; Sample 49. **5:** *Sphenolithus predistentus* Bramlette and Wilcoxon, 1967; Sample 49. **6:** *Reticulofenestra minuta* Roth, 1970; Sample 49. **7:** *Clausicoccus subdistichus* (Roth and Hay *in* Hay *et al.*, 1967) Prins, 1979; Sample 9. **8, 9:** *Helicosphaera compacta* Bramlette and Wilcoxon, 1967; Sample 9. **10:** *Helicosphaera bramlettei* (Müller, 1970) Jafar and Martini, 1975; Sample 49. **11, 12:** *Helicosphaera recta* (Haq, 1966) Jafar and Martini, 1975; Sample 49. **13:** *Helicosphaera reticulata* Bramlette and Wilcoxon, 1967; Sample 9. **14:** *Orthozygus aureus* (Stradner, 1962) Bramlette and Wilcoxon, 1967; Sample 49. **15:** *Helicosphaera euphratis* Haq, 1966; Sample 49. **16:** *Helicosphaera seminulum* Bramlette and Sullivan, 1961; Sample 49. **17:** *Zygrhablithus bijugatus* (Deflandre in Deflandre and Fert, 1954) Deflandre, 1959; Sample 9. **18:** *Coccolithus formosus* (Kamptner, 1963) Wise, 1973; Sample 9.**19:** *Pontosphaera latoculata* (Bukry and Percival 1971) Perch-Nielsen 1984; Sample 9. **20:** *Reticulofenestra umbilicus* (Levin, 1965) Martini and Ritzkowski, 1968; Sample 9. **21:** *Reticulofenestra hillae* Bukry and Percival, 1971; Sample 9. **22:** *Blackites spinosus* (Deflandre and Fert, 1954) Hay and Towe, 1962; Sample 49. **23:** *Clausicoccus subdistichus* (Roth and Hay *in* Hay *et al.*, 1967) Prins, 1979; Sample 7. **24:** *Helicosphaera compacta* Bramlette and Wilcoxon, 1967; Sample 33. **25**, **26:** *Cyclicargolithus floridanus* (Roth and Hay, *in* Hay *et al.*, 1967) Bukry, 1971; Sample 7. **27:** *Bramletteius serraculoides* Gartner, 1969; Sample 7. **28**: *Bramletteius serraculoides* Gartner, 1969; Sample 9. **29:** *Coccolithus pelagicus* (Wallich 1877) Schiller, 1930; Sample 7. **30:** *Pontosphaera multipora* (Kamptner, 1948 ex Deflandre in Deflandre and Fert, 1954) Roth, 1970; Sample 7. **31:** *Reticulofenestra lockeri* Müller, 1970; Sample 33. **32:** *Braarudosphaera bigelowii* (Gran and Braarud 1935) Deflandre, 1947; Sample 7. **33:** *Coccolithus eopelagicus* (Bramlette and Riedel, 1954) Bramlette and Sullivan, 1961; Sample 7. **34:** *Chiasmolithus altus* Bukry and Percival, 1971; Sample 33. **35**: *Zygrhablithus bijugatus* (Deflandre in Deflandre and Fert, 1954) Deflandre, 1959; sample 33. **36:** Ascidian spicule; Sample 7.

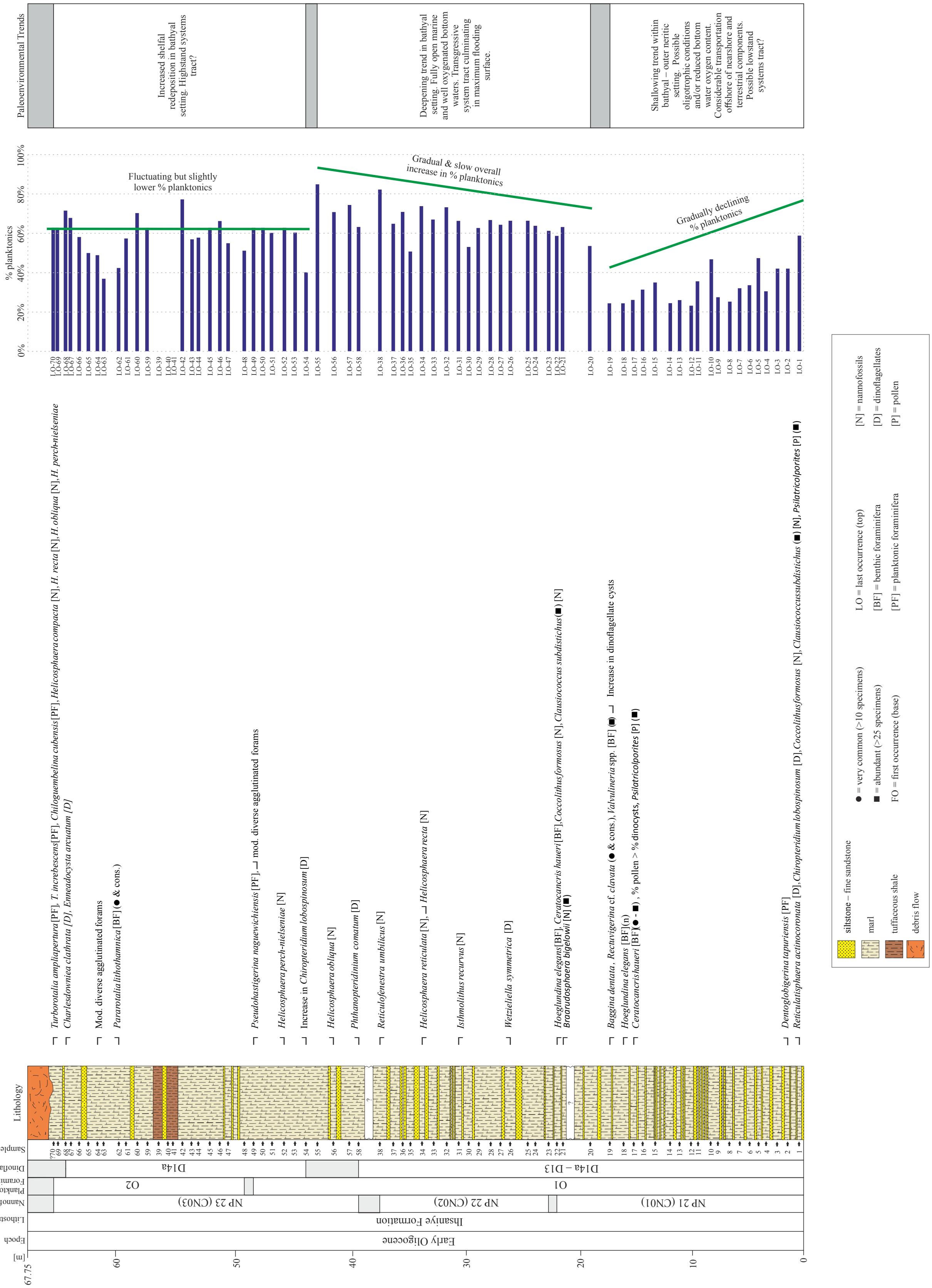

Figure 14. Key biostratigraphic events and interpretation within the İhsaniye Formation (Hanging Wall Section), Karaburun.

Eocene restricted taxa, and the presence of *Chiloguembelina cubensis* and *P. naguewichiensis* in samples 1 to 49, this part of the Hanging Wall Section can be assigned to Zone O1. The sporadic presence of *Dentoglobigerina tapuriensis* (occurring as low as sample 2) suggests that the very lowest part of the O1 Zone is not present in the studied section. The position of the FO of this species is not fully agreed, but Aze et al. (2011) and Stewart and Pearson (2000)[2] place it a little above the base of the O1 Zone. In contrast, Pearson and Wade (2015) have argued that the FO occurs within the latest Eocene of Tanzania.

7.2.2. Biozone O2

Biozone O2 is defined as the interval between the LO of *P. naguewichiensis* at its base and the LO of *Turborotalia ampliapertura* at its top (Wade et al., 2011). Based on the absence of *P. naguewichiensis* and the presence of *T. ampliapertura* in samples 48 to 70, this part of the Hanging Wall Section can be assigned to Zone O2. The absence of *Paragloborotalia opima* also suggests that this section is no younger than Zone O2. Berggren et al. (1995) placed the FO of this species approximately 300,000 to 400,000 years below the LO of *T. ampliapertura*, the marker species for the top of the O2 Zone.

The presence of *Turborotalia increbescens*—recorded only in the highest sample in the Hanging Wall Section (sample 70)—is noteworthy. The LAD of this species is placed at or close to the top of the O2 Biozone by Aze et al. (2011) and Stewart and Pearson (2000). However, in the recently published Atlas of Oligocene Planktonic Foraminifera, the authors (Wade et al., 2018) show *T. increbescens* as ranging only sporadically/rarely into the lowermost part of biozone O2. We consider our specimens (Figure 15; 10–12) to be very close to those illustrated for *T. increbescens* by Wade et al. (2018; plate 14.3); therefore, this latest information on the range of *T. increbescens* might suggest that the interval at Karaburun represented by samples 48 to 70 in the Hanging Wall Section might encompass only the lowermost part of the O2 Biozone.

7.3. Palynology

Most of the samples yielded very high abundance assemblages of variably poorly to well-preserved palynomorphs (Figure 16). The assemblages generally comprise high abundance and high diversity marine dinocysts with microforam test linings. Additionally, the miospore assemblages are generally of high abundance, with a large number of bisaccate pollen (including *Pinuspollenites* and *Podocarpidites*) derived from hinterland conifers. Rare to common *Taxodium* (swamp cypress) are derived from lowland swamps, as are fern spores (*Cyathidites*, *Laevigatosporites*, *Pteris*, and *Verrucatosporites*). Gramineae (grass pollen) are rare. The angiosperm pollen *Psilatricolporites* is particularly abundant in the lower part of the section (samples 1–17) (Figure 14), although the parent plant affinity of this taxon is uncertain. The freshwater alga *Botryococcus* is recorded as rare to common from most of the samples. Fungal spores and hyphae are generally common to very common. The overall dinocyst assemblages indicate an Early Oligocene age (see also Sancay and Batı, 2020). Occurrences of rare specimens of *Wetzeliella symmetrica* (samples 26, 30, 36, and 54) indicate an Early Oligocene age, and specimens of *Charlesdowniea clathrata* (samples 19 and 68) indicate an age within the Early Oligocene to Late Eocene. *Chiropteridium lobospinosum* is recorded in some abundance in samples 54, 53, 61, and 68, and as rare specimens from samples 45, 20, and 1. This taxon ranges no older than Oligocene.

The dinocyst *Enneadocysta pectiniformis* is recorded in variable abundance (rare to common/abundant) from all the samples, and the related *Enneadocysta arcuatum* is recorded from samples 1 to 68, also variably rare to common/abundant. These taxa have a similar recorded range of Middle Eocene to Early Oligocene (Stover et al., 1996; Williams and Bujak, 1985), while Zaporozhets and Akhmetiev (2017) record *E. pectiniformis* from the Eocene to the end of the Early Oligocene in the Northern Caucasus.

Zonal definition of the assemblages present is difficult, although the interval of abundance of *C. lobospinosum*, with associated *E. arcuatum* and *E. pectiniformis* (samples 68 to 54) provides good evidence for Zone D14a (Costa and Manum, 1988; Vandenberghe et al., 2012; Powell, 1982), while the assemblages from the lower part of the section (samples 58 to 1), which include *Reticulatosphaera actinocoronata* and *W. symmetrica*, indicate a range between zones D14a to D13 (Costa and Manum, 1988; Vandenberghe et al., 2012; Powell, 1982) (Figures 10, 14).

Zaporozhets (1999) and Zaporozhets and Akhmetiev (2017) described the palynology of the Middle Eocene–Lower Miocene at the Belaya River, Northern Caucasus, including an Early Oligocene section. While there are similarities in the assemblages recorded, abundances often differ and some taxa recorded at Karaburun are not recorded at the Belaya River section and vice versa. This might be in part because of paleoenvironmental differences and differing taxonomic concepts. The Belaya River section is the type section for the Maykop Suite (Popov et al., 2019), where the succession is dominated by black shales reflecting bottom-water anoxia in basinal conditions that are episodically brackish (Sachsenhofer et al., 2017). As discussed in the section on paleoenvironments, the Karaburun section generally represents a mostly well-

[2] Stewart DRM, Pearson PN (2000). PLANKRANGE: A Database of Planktonic Foraminiferal Ranges http://palaeo.gly.bris.ac.uk/Data/plankrange.html. In PLANKRANGE: A Database of Planktonic Foraminiferal Ranges. University of Bristol. Updated 2002.

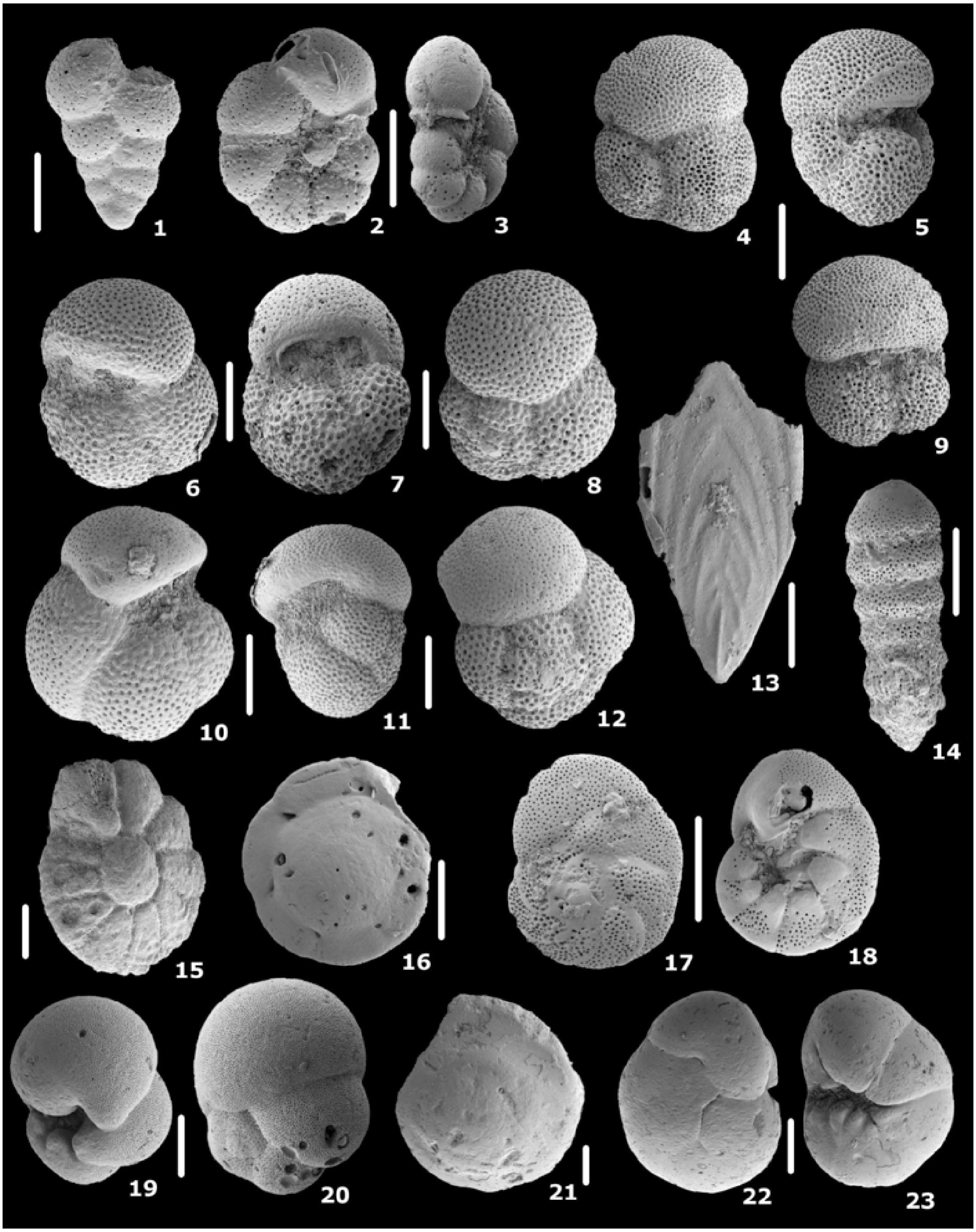

Figure 15. Key foraminifera from the Hanging Wall Section, İhsaniye Formation, Karaburun. Scale bars are each 100 µm unless otherwise stated. **1:** *Chiloguembelina cubensis* (Palmer); sample 26. Scale bar = 50µm. **2:** *Pseudohastigerina naguewichiensis* (Myatliuk); sample 13. Scale bar = 50µm. **3:** *Pseudohastigerina naguewichiensis* (Myatliuk); sample 13. Scale bar = 50µm. **4:** *Dentoglobigerina tapuriensis* (Blow and Banner); sample 21. **5**: *Dentoglobigerina tapuriensis* (Blow and Banner); sample 21 **6**: *Turborotalia ampliapertura* Bolli; sample 44. **7**: *Turborotalia ampliapertura* Bolli; sample 44 **8**: *Turborotalia ampliapertura* Bolli; sample 44. **9**: *Dentoglobigerina tapuriensis* (Blow and Banner); sample 21. **10**: *Turborotalia increbescens* Bandy; sample 70. **11**: *Turborotalia increbescens* Bandy; sample 70. **12**: *Turborotalia increbescens* Bandy; sample 70. **13**: *Frondicularia tenuissima* Hantken; sample 12. **14**: *Rectuvigerina* cf. *clavata* (Franzenau); sample 12. **15**: *Pararotalia lithothamnica* (Uhlig); sample 69. **16**: *Oriodorsalis umbonatus* (Reuss); sample 4. **17**: *Valvulineria complanata* (d'Orbigny); sample 19. **18**: *Valvulineria complanata* (d'Orbigny); sample 19. **19**: *Baggina dentata* Hagn; sample 4. **20**: *Baggina dentata* Hagn; sample 4. **21**: *Hoeglundina elegans* (d'Orbigny); sample 18. **22**: *Ceratocancris haueri* (d'Orbigny); sample 7. **23**: *Ceratocancris haueri* (d'Orbigny); sample 7.

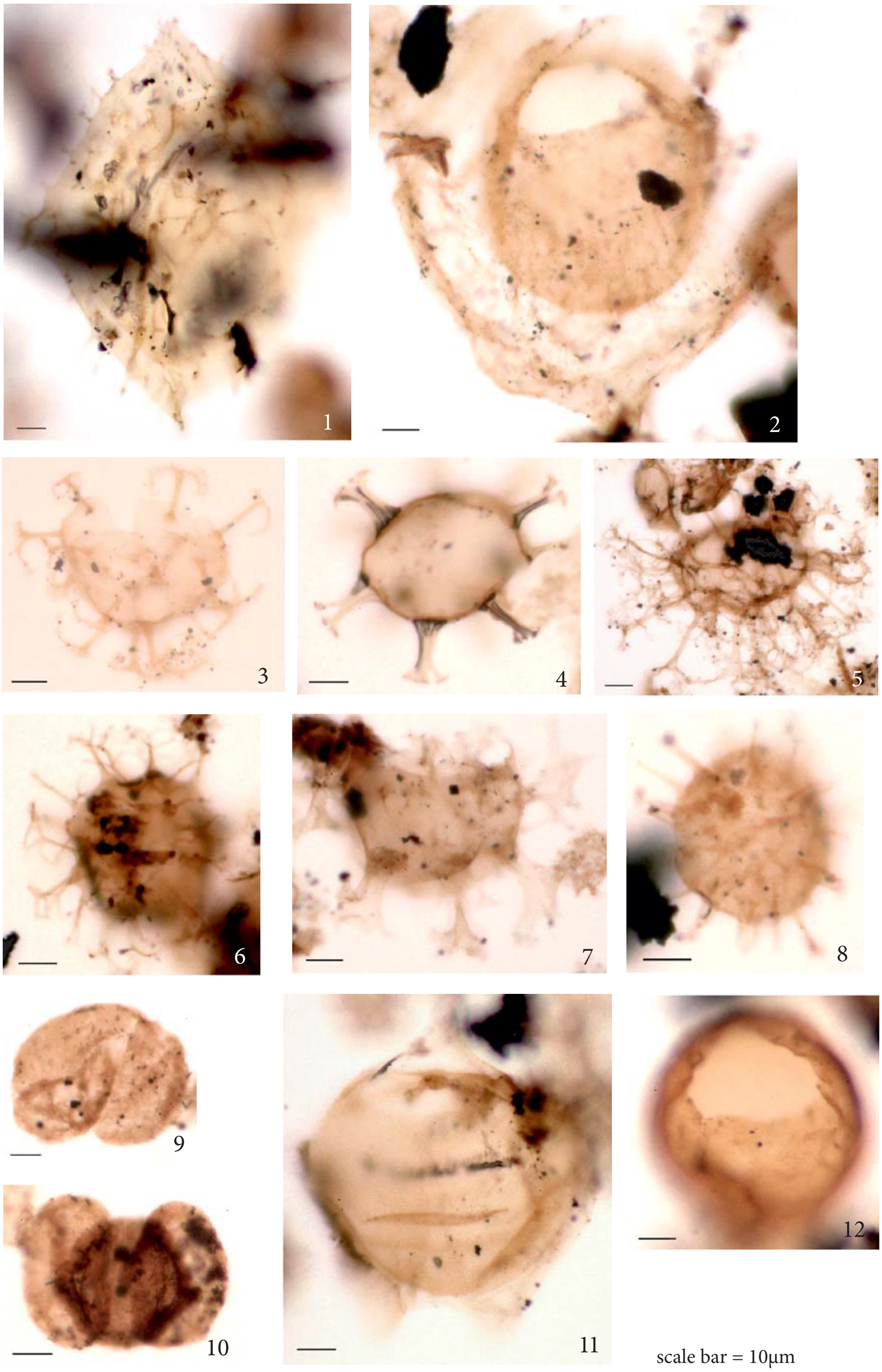

Figure 16. Representative palynomorphs from the Hanging Wall Section, İhsaniye Formation, Karaburun. **1:** *Charlesdowniea clathrata* Sample 19. **2:** *Thalassiphora pelagica* Sample 68. **3:** *Enneadocysta pectiniformis* Sample 54. **4:** *Homotryblium plectilum* Sample 54. **5:** *Reticulatosphaera actinocoronata* Sample 58. **6:** *Spiniferites* sp. Sample 68. **7:** *Chiropteridium lobospinosum* Sample 54. **8:** *Operculodinium* sp. Sample 61. **9:** *Pinuspollenites* sp. Sample 45. **10:** *Podocarpidites* sp. Sample 45. **11:** *Deflandrea phophoritica* Sample 68. **12:** *Batiacasphaera* sp. Sample 61.

oxygenated outer shelf to slope succession. The Belaya River section lies to the north of the Greater Caucasus and was thus deposited in a basin separate from the Black Sea Basin (Vincent and Kaye, 2018; Sachsenhofer et al., 2017). This might also account for differences between the palynological assemblages.

Gürgey and Batı (2018) recently described the palynology of the Mezardere Formation in the Thrace Basin. They used the presence of *Glaphyrocysta* cf. *semitecta* and *Wetzeliella gochtii* to indicate an Early Oligocene age (after Williams et al., 2004; Pross et al., 2010) and thus age equivalence with the İhsaniye Formation. An interval with common *G. semitecta* was observed within the lower part of the İhsaniye Formation at Karaburun which lies within the range NP21 to NP22, thus supporting their age interpretation. *W. gochtii* was not noted in our study and the genus *Wetzeliella* was rare, while it appears to be abundant in the upper Mezardere Formation. This might relate to a more coastal depositional position with increased coastal sea surface productivity brought on by sediment/nutrient runoff.

7.4. Integrated conclusions

All three biostratigraphic disciplines employed suggest that the studied section can be biostratigraphically calibrated to the Early Oligocene (Rupelian) (Figure 14). Calibration of the biozones present to the chronostratigraphic standard as indicated by Vanderberghe et al. (2012) (Figure 10), suggest that the section is no older than 33.9 Ma and no younger than 30.5 Ma (i.e. it encompasses the lower half of the Rupelian). In addition to biostratigraphic data, we have obtained radiometric age data determined from zircons in acidic tuffs interbedded within the İhsaniye Formation. Although these data are not from the Karaburun section, instead coming from localities to the south and northwest, they provide further useful age constraints on the formation. Zircon U-Pb ages of 33.9 (±0.4) Ma (Kıyıköy locality; Okay et al., 2020), 32.5 Ma, 31.7 Ma, and 31.04 Ma (localities to the south of Karaburun; Okay et al., 2019) have been recorded, all of which are compatible with the age determination of the Karaburun section (age calibration model of Sahy et al., 2017).

Biostratigraphic data demonstrate that the hanging wall stratigraphy of the İhsaniye Formation is relatively complete, encompassing approximately the lower half of the Rupelian (Early Oligocene), with calcareous nannofossil zones upper NP21 to lower NP23 and planktonic foraminiferal biozones O1 (~P18) and O2 (~P19) present. By contrast, the footwall section is restricted to NP23, suggesting that a now inverted normal fault controlled deposition in Early Oligocene time. Deposition of older stratigraphy was restricted to the hanging wall, with deposition commencing on the footwall during NP23, initially with pebbly sandstones, subsequently with marls.

Within the footwall section the presence of *N. bouillei* confirms an Early Oligocene age, but no age-diagnostic planktonic foraminiferal taxa were found, particularly no evidence for the O1 standard planktonic foraminiferal biozone. This can be identified by the presence of *P. naguewichiensis*, which was recorded in the lower part of the Hanging Wall Section. Calcareous nannofossil data places all İhsaniye Formation samples from the Footwall section in Biozone NP23 (Subzone CNO3), so it should be expected that samples from the Footwall Section would correspond to O2 (= P19) standard planktonic foraminiferal zone. Whilst we have been unable to replicate their results, Okay et al. (2019) noted P19 planktonic foraminifera in their samples from the higher calcareous marls onlapping the Soğucak Formation.

According to Vanderberghe et al. (2012), the boundary between planktonic foraminiferal zones O1 and O2 and the boundary between calcareous nannofossil zones NP22 and NP23 might be synchronous (Figure 10). We have not determined that to be the case in the studied section (Figure 14). At Karaburun, the boundary between O1 and O2 lies significantly above the boundary for NP22 and NP23 (i.e. O1 indicative planktonic foraminifera are found in some samples that contain NP23 indicative calcareous nannofossils). This result might be significant for the ongoing calibration between biostratigraphy schemes for the Early Oligocene.

8. Micropaleontological determination of paleoenvironments

Microfossils can provide useful information concerning depositional settings and stratigraphic trends in paleoenvironment. The fine-grained, marly nature of much of the İhsaniye Formation within the studied section suggests relatively low energy deposition, with episodically high-energy events represented by sharp- or erosive-based sandstones, limestones, and debris beds. A key question is if this style of deposition is taking place on a paleoshelf, on a paleoslope, or within the deeper basin.

The depositional setting of the Hanging Wall Section and footwall section are considered separately.

8.1. Hanging Wall Section

8.1.1. Foraminiferal data

Apart from the three samples that are barren or contain only very impoverished microfauna, all samples are very rich and very diverse and comprise abundant planktonic and calcareous benthic foraminifera. Agglutinated foraminifera are relatively less common, but local influxes are recorded sporadically.

The relative percentages of planktonic foraminifera are consistently high (Figure 14), indicating deposition in fully marine conditions (with at least good connections to the open ocean) and well-oxygenated surface waters. Dilution of surface water salinity by fresh-water run-off appears to have been minimal.

Percentages of planktonic foraminifera appear to exhibit a moderate decline from approximately 60% at the base of the section in sample 1, to approximately 25% in sample 19. From sample 20 to the top of the section, the interval can be further subdivided based on a gradual but somewhat erratic upwards increase in percentages of planktonic foraminifera from approximately 60% to approximately 80% between samples 20 and 55 and with slightly lower but steadily fluctuating percentages from sample 54 to the top of the section.

In the lower part of the section, this trend may indicate some shallowing from possible upper bathyal to outer neritic paleowater depths although above sample 20 paleowater depths were probably wholly bathyal (i.e. greater than approximately 200 m). The gradual deepening trend between samples 20 and 55 might represent transgressive conditions culminating in a maximum flooding surface at approximately the level of sample 55 (see Figure 14 and subsequent paragraphs).

The compositional change between samples 19 and 20 is also marked by a distinct shift in the composition of the benthic foraminiferal microfaunas above and below this level. *Hoeglundina elegans* is very abundant within the lower interval, sometimes reaching counts of well over 100 specimens in a sample. Additionally in this lower interval, several taxa are consistently common to abundant whereas they are much more sporadically recorded in higher samples and in much fewer numbers. These include *Baggina dentata*, *Ceratocancris haueri*, *Frondicularia tenuissima*, *Oriodorsalis umbonatus*, *Rectuvigerina* cf. *clavata*, *Valvulineria complanata*, and *Valvulineria palmarealensis*.

Hoeglundina elegans is an aragonitic species that ranges from Late Eocene to Recent. It is generally a neritic to bathyal taxon that prefers deeper oxygenated bottom waters, but with oligotrophic (low nutrient) conditions. However, it is also known to tolerate low oxygen conditions, for example in the Californian borderland basins (Mackensen and Douglas, 1989). Therefore, it is possible that the lower part of the section represents a period of reduced bottom water oxygen content and/or a period of extreme oligotrophic conditions similar to those that exist in the present day Eastern Mediterranean (Ní Fhlaithearta et al., 2010). For the latter case, it has been demonstrated that *H. elegans* can migrate into shallower (shelfal) waters during periods of extreme oligotrophy, though perhaps in lower numbers. On the other hand, the abundance and diversity of microfaunas recorded in all but the three barren/impoverished samples suggests that eutrophic environments predominated throughout deposition.

In the upper part of the section, the distinctive species *Pararotalia lithothamnica* is recorded sporadically but becomes (relatively) consistent and occasionally abundant from sample 62 to sample 70. Given that this part of the section contains increasing evidence for debris flows, it is possible that this species is being reworked from shelfal (neritic) environments into bathyal conditions.

Agglutinated foraminiferal taxa are recorded fairly consistently throughout the section and display variable and changing abundances. However, there is an interval between samples 49 and 64 where the diversity of such forms appears to be somewhat higher. This might relate to an interval of decreasing dissolved oxygen. The percentage of agglutinating taxa in the overall foraminiferal assemblages is very low (mostly <5%) and only exceeds 10% in one sample (48).

8.1.2. Palynological data

Overall, the high abundance of dinocysts such as *Enneadocysta*, *Homotryblium*, *Spiniferites*, and *Operculodinium* suggests a fully open marine, possibly shelfal setting.

Samples 1 to 17 have a somewhat different character from samples that lie above these. Dinocysts are relatively less common as a proportion of the assemblage and spores and pollen are relatively common. The angiosperm pollen *Psilatricolporites* is particularly common within this lower section. From sample 20 upwards, dinocysts (particularly *Enneadocysta* and *Spiniferites*) become consistently relatively common and might reflect a transgressive trend to more open marine conditions.

A further change is recorded from sample 54 and above, with a marked increase in *C. lobospinosum,* suggesting a shallowing toward shelfal settings, or increased redeposition from shelfal to more offshore environments (Sluijs et al., 2005; Williams et al., 2009). A marked increase in the dinocyst diversity in sample 54 might also be associated with this change in depositional environment.

8.1.3. Calcareous nannofossil data

Abundance and diversity patterns of calcareous nannofossils, which had a widespread oceanic distribution and lived within the photic zone, can provide important information concerning paleoenvironment, such as nutrient supply, water temperature, salinity changes.

Abundant and well-preserved calcareous nannofossils assemblages throughout the investigated section point to a normal salinity marine environment. All assemblages are dominated by *C. floridanus* and *R. minuta*. High numbers of eutrophic species such as *C. floridanus* point to a stable nutrient supply within a well-stratified, marine water column.

Haq (1980) concluded that small reticulofenestrids dominate nannoplankton assemblages along continental margins. *R. minuta* is a very small (<3 μm) elliptical reticulofenestrid with a long stratigraphic range from the lower Eocene (NP13) to Pliocene. Blooms of *R. minuta* in Miocene sediments from Central Paratethys have been interpreted as indicators of a warmer, better-stratified water column compared to other assemblages with a dominance of *C. pelagicus* (Ćorić and Hohenegger, 2008). In contrast, discoasterids, which are common in open and deep oceanic water (Aubry, 1992) are well preserved throughout the studied section, but occur only very sporadically.

Most samples also contain a high diversity of helicoliths (*H. bramlettei*, *H. compacta*, *H. euphratis*, etc.) and cribriliths (*P. multipora*, *P. latoculata*, *P. formosa,* etc.). Assemblages of *Helicosphaera* and *Pontosphaera* exhibit more diversity nearshore than in open oceanic conditions (Aubry, 1990).

C. pelagicus is an important paleoecologic marker because it indicates higher nutrient levels and eutrophic conditions usually caused by upwelling (Okada and McInyre, 1979; Winter et al., 1994). A relative abundance of *C. pelagicus* within the lower part of the section (samples 1 to 31; NP21 to lowerNP22) points to higher nutrient input and probably more turbulent water caused by more intense fresh-water runoff.

The relative high abundance of *C. pelagicus* within this part of the section cooccurs with a relative high abundance of *Braarudosphaera bigelowii* (particularly in samples 1 to 21; NP21). Bukry (1974) investigated changes in the abundance of this species during the Holocene in Black Sea sediments and concluded that they reflect fluctuations in water salinity. High abundances can be associated with a salinity reduction. The occurrence of common ascidian spicules and plant remains in samples 1 to 26 (NP21 and lower part of NP22) suggests relatively shallow conditions compared to the upper part of the section.

8.1.4. Integrated paleoenvironmental conclusions: Hanging Wall Section

All fossil groups studied indicate that the Hanging Wall Section can be subdivided into distinctive lower and upper parts (Figure 14).

Overall, sample 20 and above contains rich assemblages of planktonic and benthonic foraminifera and dinocysts (dinocyst increase from sample 19) and might reflect deposition in fully open marine, well-oxygenated, eutrophic, bathyal conditions (nannofossil abundance also supports this, but the taxa present do not suggest fully open oceanic conditions). Nannofossil assemblages dominated by small reticulofenestrids (*R. minuta*) and *C. floridanus* suggest a continental margin depositional setting and a eutrophic, better-stratified water column than within the lower part of the section. Reworking of shelfal fauna and flora is noted within the highest samples (sample 53 and above and particularly sample 62 and above).

Samples 1–19 contain relatively less common planktonic foraminifera, and samples 1–18 contain less common dinocysts, and some benthonic foraminifera indicative of slightly shallower environments. Relative pollen and spore abundance might support this notion or at least offshore transportation of nearshore and terrestrial components. There are indications (i.e. abundance of the benthonic foraminifer *H. elegans*) that bottom waters might be reduced in oxygen content and/or oligotrophic. Similarly, shallower environments with high nutrient supply and perhaps traces of a freshwater plume from a point source are demonstrated by calcareous nannofossils assemblages with a relatively high abundance of *C. pelagicus* coupled with *B. bigelowii*. Common ascidians and transported plant remains within this part of the sections support this assumption.

In summary, the Hanging Wall Section at Karaburun most likely represents deposition in an outer neritic (shelf)–bathyal (slope) depositional setting. A shallowing upwards trend is evident within the lower part of the succession (samples 1–19) and this may represent a depositional lowstand. This interval, in the earliest Oligocene part (i.e. Biozones NP21/O1) might have experienced bottom water dysoxia and/or oligotrophy. The highest organic carbon content occurs within this lower part of the section (Tulan et al., 2020) indicating bottom-water conditions conducive to the preservation of organic matter. Above this, the succession is transgressive in nature between samples 20 and 55, based on planktonic foraminifera abundance and the presence of dominant fine grained lithologies, with a maximum flooding surface being present at around sample 55. Above this, from sample 54–70, increased shelfal redeposition into an overall bathyal environment is noted; this might represent highstand depositional settings.

8.1.5. Benthic foraminifera morphogroup distribution patterns

The calcareous benthic foraminiferal data from the Hanging Wall Section have been analyzed on the basis of grouping species from the same genus together and sometimes grouping morphologically similar genera together to form artificial "morphogroups". This approach has been used by some authors (e.g., Jones and Charnock, 1985) to relate test shape to different feeding strategies and other related environmental factors. However, for this particular study we have attempted to relate the proportions of different morphogroups in assemblages to particular systems tracts as determined by the paleobathymetric trends, as discussed in the previous section (Figure 14).

The morphogroups analyzed which displayed some degree of apparent relationship include:

· *Anomalina*/*Anomalinoides* (robust, low trochospiral/planispiral)

· *Astacolus/Marginulina/Vaginulinopsis/Percultazonaria* (uncoiled/partly uncoiled rectilinear lenticulinids)

· *Baggina/Cancris/Ceratocancris* (thin-walled, low trochospiral)

· *Bolivina/Loxostomum/Lingulina* (biserial, elongate)

· *Chilostomelloides*

· *Cibicides/Lobatula/Discorbis/Hanzawaia* (plano-convex, low trochospiral)

· *Cibicidoides*

· *Hoeglundina*

· *Lagena*

· *Lenticulina/Saracenaria* (lenticular planispiral)

· *Melonis/Pullenia* (rounded planispiral)

· *Pararotalia* + "Larger" Foraminifera (nummulitids)

· Polymorphinids

· *Uvigerina/Angulogerina/Trifarina/Reussella/Rectuvigerina/Siphogenerinoides* (multiserial, elongate)

· *Valvulineria*

The percentage proportions of each morphogroup for every sample are graphically displayed in Figures 17–19. Each systems tract has been highlighted: samples 1 to 19 (lowstand systems tract - LST); 20 to 55 (transgressive systems tract - TST) and 54 to 70 (highstand systems tract - HST) (note sample 54 occurs *above* sample 55 in the field).

It is noticeable that some morphogroups display positive or negative correlation with particular systems tracts, others part-positive or part-negative correlation. In some places the differences are evident (e.g., *Lagena* in the TST or *Hoeglundina* in the LST), and in others, the differences are more equivocal (e.g., *Cibicidoides* in the HST or Polymorphinids in the TST). Also shown on each morphogroup chart is a line delineating the mean percentage composition within that particular systems tract.

Some morphogroups display little or no discernable pattern and are not shown. These include *Bulimina/Ceratobulimina/Praeglobobulimina*; *Elphidium/Elphidiella/Nonion/Nonionella*; *Globocassidulina*; *Gyroidinoides* and "Uniserial elongate types (e.g., dentalinids *sensu lato*)".

For some cases a causal relationship could be inferred. For example, the high proportion of *Hoeglundina* in samples from the LST are probably related to conditions of lower oxygen levels in a stratified water column, or the presence of deeper water taxa (e.g., *Melonis*, *Lagena* and lenticulinids) in the TST, or the presence of shallow-water forms (e.g., *Pararotalia* and "larger" benthics in the upper–shallower parts of the HST. Other relationships, although displaying a discernable positive or negative correlation with a particular systems tract, are less easily linked to a possible cause (e.g., the previously discussed apparent preference of *Lagena* for TST conditions but with similarly higher proportions in the upper part of the HST).

In isolation, the use of graphic displays for individual morphogroups might not provide a great deal of useful information, but examining several separate groups together suggests that morphogroup analysis is useful for characterizing depositional systems tracts. The use of morphogroups may also help to mitigate against restrictions in interpretation caused by using particular time-specific taxa or species/genera that are prone to taxonomic misunderstanding. Whilst we may not fully understand why certain morphogroups are indicative of either transgressive or regressive conditions, the empirical relationships are undeniable and provide an interesting context for more detailed studies in the future.

8.2. Footwall section

8.2.1. Foraminiferal data

8.2.1.1. Pebbly sandstone facieS

The lowest 20 m of exposed stratigraphy within the Footwall Section is dominated by coarse pebbly sandstones. However, thin (typically <10-cm thick), often discontinuous calcareous siltstones and marls occur within this facies, sampled for their foraminiferal content in disaggregated preparations (see Section 5). Additionally, thin sections were prepared from suitable calcareous siltstones and sandstones.

In disaggregated preparations, assemblages are dominated by diverse calcareous benthic foraminifera and generally low proportions of planktonic foraminifera (20–30% gradually increasing upwards to a peak of approximately 40%). Assemblages are dominated by Cibicidids and Lenticulinids. Bolivinids (mainly of the *Bolivina beyrichi* group) are also moderately common and consistent.

Influxes of *Nummulites bouillei* are recorded. These coincide with the lowest proportions of planktonic foraminifera in this subset and indicate proximity to shallow waters, if not the actual paleodepths where *Nummulites* flourish then close to them.

Thin sections of calcareous sandstone samples contain occasional *Nummulites* and possible *Lepidocyclina*, as well as sporadic globigerinid planktonic foraminifera, possibly *Dentoglobigerina*.

Overall, deposition is thought to have occurred in inner-mid shelfal water depths with a well-oxygenated water column.

8.2.1.2. Lower calcareous marls

The coarse pebbly sandstone facies at the base of the section passes up into approximately 50 m of marl with approximately 5 m of the lower section accessible in the cove that within the core of a small syncline to the north of the inverted normal fault. Assemblages from this set of samples have a slight dominance of planktonic foraminifera (50–60%) except in the lowest sample which

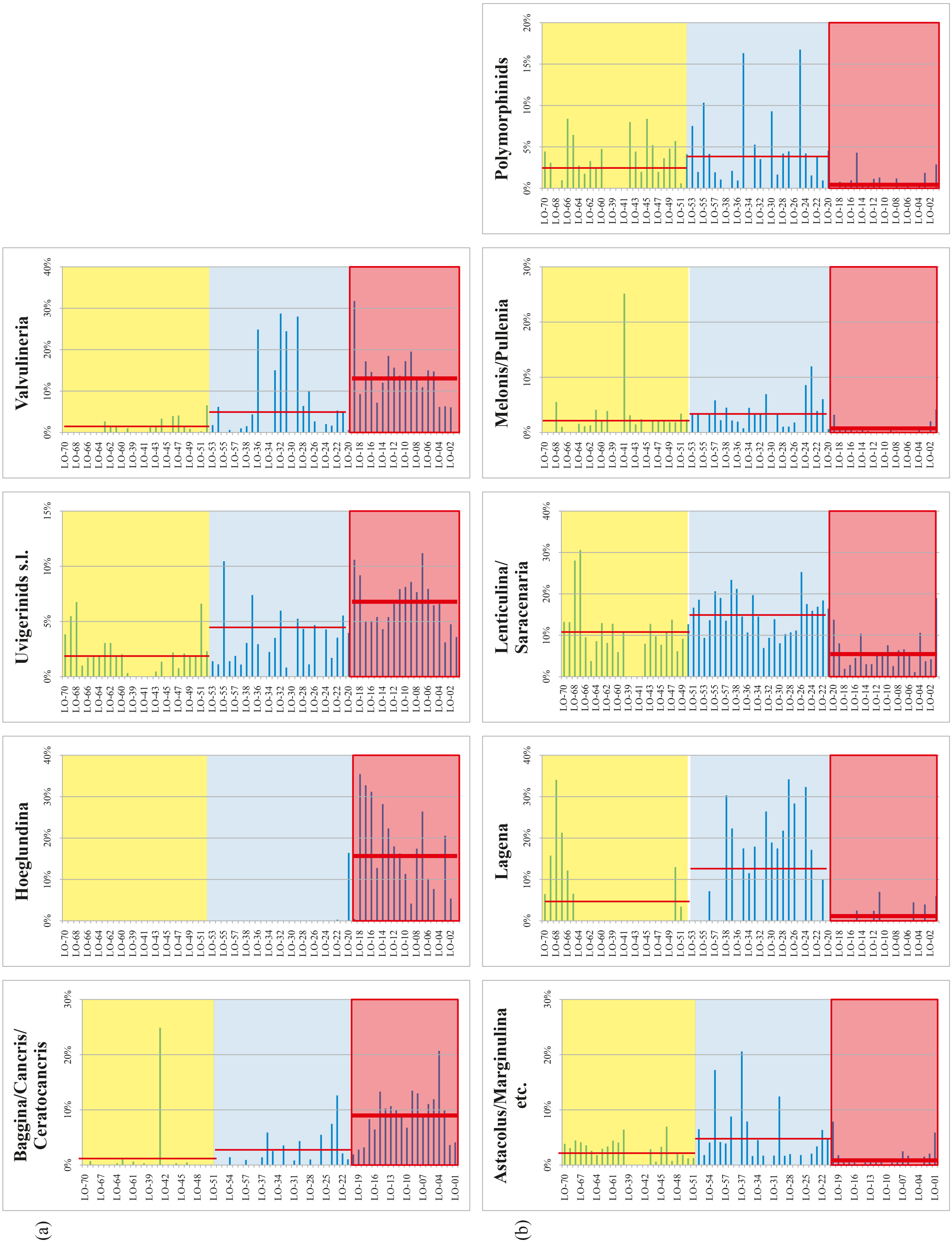

Figure 17. Benthic foraminiferal morphogroups that appear to show (a) positive and (b) negative correlation with lowstand, low oxygen environments (boxed, pink zone). Scales are percentages of that morphogroup present in each assemblage with red lines showing the mean value in each systems tract.

is calcareous benthic dominated (only 20% planktonics). Benthic assemblages are dominated by Cibicidids and Lenticulinids. An informally named taxon *Cibicidoides* sp. 1 is moderately common to common. *Cibicidoides* aff. *tenellus* is very common in one sample. Additionally, bolivinids (mainly of the *B. beyrichi* group) are moderately common and consistent and reach maximum abundances within this set of samples. *Reussella oberburgensis* is generally moderately common within this subset. *Tritaxia szaboi*, a characteristic large agglutinated foraminifera, is very common.

The biserial planktonic foraminifera *Chiloguembelina cubensis* is common to very common, reaching its maximum abundance within this set of samples.

A large influx of *N. bouillei* is recorded in one sample high in the stratigraphy. This influx coincides with a planktonic foraminifera proportion of approximately 60%, which indicates relatively deeper waters (outer shelf - ?upper bathyal). The *Nummulites* here have almost certainly been introduced into these sediments by downslope transport.

Overall, deposition is thought to have occurred in outer shelfal (to possibly upper bathyal) water depths with a well-oxygenated water column.

8.2.1.3. Higher calcareous marls

The highest İhsaniye Formation within the footwall section are the marls that onlap and infill the eroded surface of the Soğucak Formation around Cape Karaburun. Several spot samples were collected from these marls.

Foraminiferal assemblages from these samples are dominated by diverse calcareous benthic foraminifera and generally low proportions of planktonic foraminifera (20–30% although with a peak of approximately 40%). Assemblages are dominated by Cibicidids and Lenticulinids with uniserial types relatively more diverse. Additionally, bolivinids (mainly of the *B. beyrichi* group) are moderately common and consistent. *T. szaboi* is relatively poorly represented within this subset except for a moderate influx in one sample.

Overall, deposition is thought to have occurred in mid shelfal water depths with a well-oxygenated water column.

9. Discussion

9.1. Stratigraphic synthesis

The new biostratigraphic data gathered within this study elucidates the depositional history of the İhsaniye Formation at Karaburun. There is clear evidence that a normal fault controlled deposition during the Early Oligocene, considering the stratigraphy on either side of this fault is quite different (Figures 5 and 9).

Towards the end of the Priabonian, deposition of the Soğucak Formation limestones ceased, and a relative sea-level fall led to the exposure and erosion of these carbonates, with the paleoreef exposed at Cape Karaburun forming a topographic high. Based on seismic evidence within the Western Black Sea (see, for example, the formation of canyons incising the shelf of the Western Black Sea (Dinu et al., 2005; Mayer et al., 2018)), Tari et al. (2014, 2019) discussed the likelihood of a major relative sea-level draw-down at, or close to, the end of the Eocene. This might be eustatically-controlled as the latest eustatic models (Miller et al., in press) show an approximately 100-m fall in the latest Eocene as a response to the onset of extensive Antarctic glaciation. Whatever the driving mechanism, this fall would have been sufficient to expose the lithified Soğucak Formation, and temporally ceased deposition within the vicinity of Karaburun. Deposition recommenced in Karaburun only on the south, downthrown, side of the (now inverted) normal fault that lies on the south side of Cape Karaburun (Figure 2). The timing of the recommencement of deposition is uncertain because the basal contact of the İhsaniye Formation is not observed on the hanging wall side of the fault. The oldest sediments exposed are low in the Early Oligocene (Biozone NP21, Subzone CNO1 (nannofossils); O1 (planktonic foraminifera)), but perhaps not at the very base of the Oligocene. The oldest İhsaniye Formation regionally might even extend into the very latest Eocene (Okay et al., 2019); however, a reassessment of their planktonic foraminiferal data (e.g., presence of *Globigerina praebulloides*, *Dentoglobigerina tripartita*, *Dentoglobigerina venezuelana*, and *Tenuitella gemma*) suggests that their sections interpreted as Late Eocene could equally be Early Oligocene. Regardless of this uncertainty, deposition appears to have recommenced close to the Eocene/Oligocene boundary, suggesting that the break in deposition caused by the sea-level fall was short in duration.

While marls with variable organic content (Tulan et al., 2020) and calcareous siltstones and occasional sandstones (of debris flows origin) were being deposited during Biozone NP21 and NP22 times in the hanging wall of the fault, no deposition was taking place on the footwall. There, deposition was initiated with the coarse pebbly sandstones, passing up into marls, both of which onlap the Soğucak Formation. These onlapping sediments are demonstrably assignable to calcareous nannofossil Biozone NP23 (Subzone CNO3) and demonstrate a rise in sea-level at this time which eventually flooded the exposed reef with deposition in erosional depressions. At the same time as the footwall side of the fault was being drowned, the hanging wall side of the fault demonstrates evidence for transgression, with a maximum flooding surface (based on plankton abundance) occurring within Biozone NP23. The transgression onto the formally exposed Soğucak reef on the footwall might have created erosion that caused the deposition of debris flows, blocks of Soğucak limestone

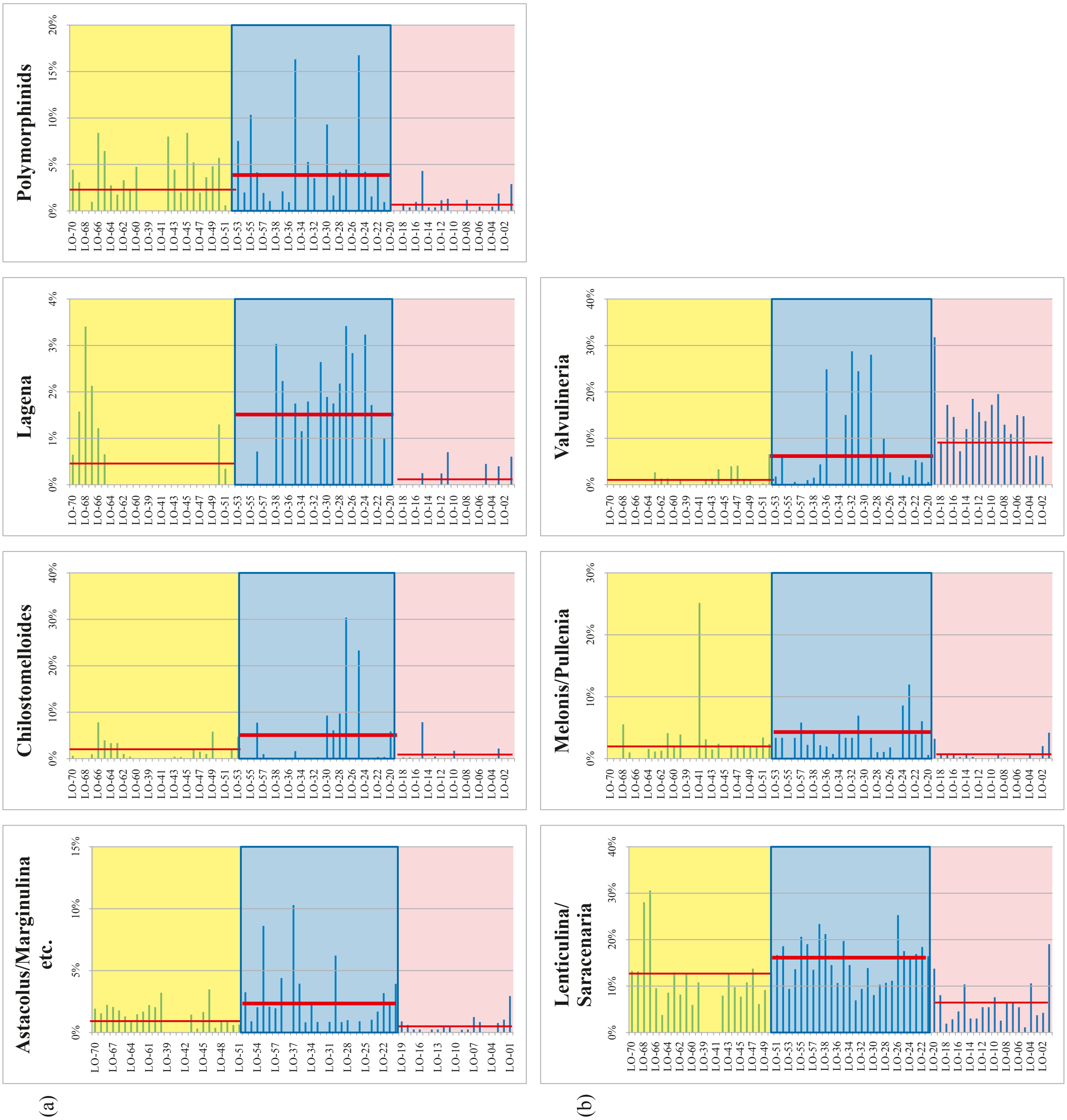

Figure 18. Benthic foraminiferal morphogroups that appear to show (a) positive and (b) part-positive correlation with transgressive environments (boxed, blue zone). Scales are percentages of that morphogroup present in each assemblage with red lines showing the mean value in each systems tract.

and slumping within the upper İhsaniye Formation in the hanging wall.

Between the Early Oligocene and present day, the fault controlling deposition became overprinted by a transpressive fault and NP21 sediments of the lower İhsaniye Formation on the hanging wall were upthrown into juxtaposition with NP23 sediments of the footwall as now observed at beach level (Figures 2, 5, and 9). The transpression has created steep dips in the proximity of the fault and the formation of a small syncline to the north of the fault (Figure 2).

Samples of the İhsaniye Formation from Karaburun have been analyzed for their Strontium isotope ratios (Sr^{86}/Sr^{87}); results are presented separately (Tulan et al., in press).

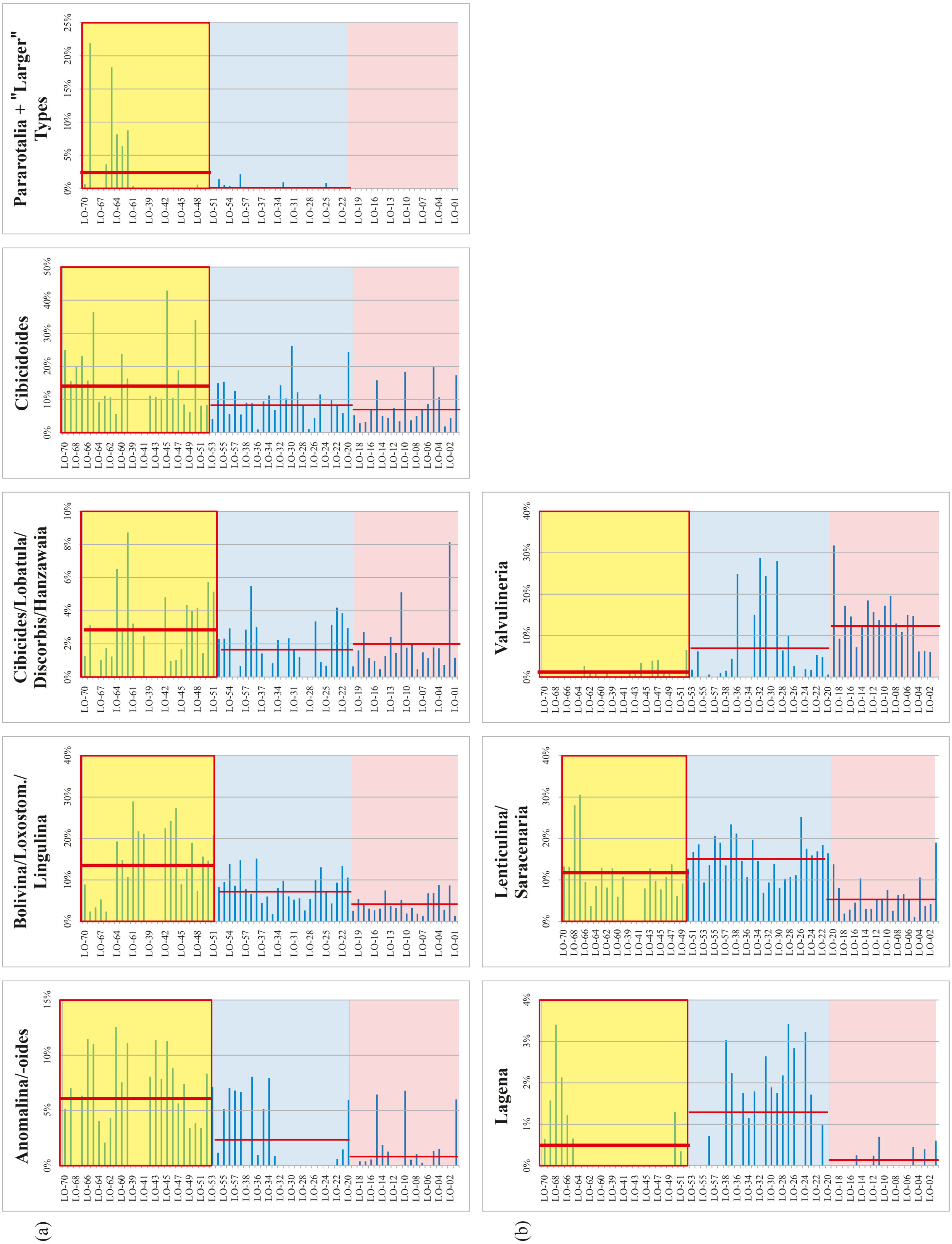

Figure 19. Benthic foraminiferal morphogroups that appear to show (a) positive and (b) part-positive or negative correlation with highstand environments (boxed, yellow zone). Scales are percentages of that morphogroup present in each assemblage with red lines showing the mean value in each systems tract.

However, it is evident that they substantiate the Early Oligocene stratigraphic evolution as presented herein.

9.2. Regional significance

9.2.1. Lithological comparison

Much of the marly Early Oligocene section at Karaburun represents an open marine, mostly outer neritic–bathyal, depositional setting, mostly well oxygenated, with evidence for reduced bottom water oxygen conditions within its lower part. It contains abundant, diverse, and remarkably well-preserved microfaunas and microfloras of foraminifera, calcareous nannofossils, and palynomorphs. This exceptional faunal recovery and the marly, calcareous nature of its background lithology, makes the Karaburun section somewhat unique compared to coeval sections from around the Western Black Sea Basin. For example, the Ruslar Formation, exposed on the Bulgarian coast near the village of Galata, is clay-rich and includes diatomites, as well as erosively based sands and conglomerates (Suttill, 2009). This same formation is carbonate-poor within offshore wells (Sachsenhofer et al., 2009).

The Early Oligocene portion of the Maykop Suite at its type locality on the north side of the Greater Caucasus has been well documented (Popov et al., 1993; Akhmetiev et al., 1995; Zaporozhets, 1999; Saint-Germès et al., 2000; Zaporozhets and Akmetiev, 2017; Sachsenhofer et al., 2017; Popov et al., 2019). The relevant section is approximately 200-m thick, much thicker than at Karaburun, and consists of the Pshekha, Polba and Morozkina Balka formations. Much of this section consists of dark-gray clays, and carbonate content is very limited. Nannofossil zones NP21, NP22, and NP23 are recognized along with modified palynological zones D13, D14, and D15 of Costa and Manum (1988). Reworking of Eocene and older palynomorphs can be common. Ostracods and palynomorphs indicate that deposition took place in episodically brackish surface water conditions. Nonetheless, water depths might have been substantial. Based on the presence of fossil fish with photophores and the disappearance of aragonitic-shelled pteropods, Sachsenhofer et al. (2017) and Popov et al. (2019) estimate that water depths might have been as great as 1000 m, much greater than might be estimated at Karaburun. Unlike at Karaburun, deposition was more consistently anoxic. It is evident that the typical Maykop Suite bears little analogy to the age equivalent strata at Karaburun.

Some uncertainty exists around the age-equivalent stratigraphy within the Thrace Basin because significant differences exist in interpretations of age and use of local lithostratigraphic units. In a recent interpretation, Gürgey and Batı (2018) used dinocysts to provide age control on the Mezardere Formation (see also Turgut and Eseller, 2000), which they interpreted as at least partly Early Oligocene and therefore equivalent to the İhsaniye Formation. Their biostratigraphic interpretations appear valid, using the presence of *Glaphyrocysta* cf. *semitecta* and *Wetzeliella gochtii* to demonstrate an Early Oligocene age (equivalent to calcareous nannofossil biozones NP21-NP23/NP24). The Mezardere Formation is well exposed in large clay quarries south of Tekirdağ and consists mostly of dark shale, regarded as prodelta shales, with some shale oil potential. The organic enrichment exhibits some similarities to the lower part of the İhsaniye Formation at Karaburun; however, overall, the Mezardere Formation appears to have been deposited within a more restricted, less open marine environment.

9.2.2. Salinity events

In several parts of Paratethys, the onset of intra-Early Oligocene nannofossil Zone NP23 corresponds to a significant reduction in marine salinity (e.g., Budilová et al., 1992; Popov et al., 1993) as determined by distinctive blooms of dinocysts and acritarchs (*Hystrichokolpoma*, *Batiascasphaera sphaerica*, *Horologinella)*, calcareous nannofossils (*Reticulofenestra ornata*, *Transversopontis fibula*, *Transversopontis latus*), ostracods (*Disopontocipris oligocaenica*) and molluscs (*Janschinella*, *Lenticorbula*). These assemblages occur in the type Maykop Suite section on the northern side of the Greater Caucasus (Popov et al., 1985; Voronina and Popov, 1984; Sachsenhofer et al., 2017; Popov et al., 2019) and the nannofossil assemblage ("Polbinian-type nannoflora") has been seen in the Caucasus and other parts of Central and Eastern Paratethys, even as far east as the north Ustyurt Plateau between the Caspian and Aral seas and as far west as the Bavarian Foreland Molasse (Nagymarosy and Voronina, 1993; Melinte-Dobrinescu and Brustur, 2008). This "Solenovian" event is said to be widespread throughout Paratethys (Popov et al., 2002; Popov and Stolyarov, 1996; Sachsenhofer et al., 2018) and has been detected in the Bulgarian Western Black Sea (Sachsenhofer et al., 2009, 2018; Mayer et al., 2018) and in central Paratethys (Popov et al., 1993; Rusu, 1999; Schulz et al., 2004, 2005; Ozsvárt et al., 2016). Solenovian is a local stratigraphic term employed within the Caucasus region, and the Polbinian is a horizon within this, also called Ostracod Beds on account of the abundance of large-sized ostracods at this level. Despite the relative proximity to the occurrence of the Solenovian event in offshore Bulgaria (Sachsenhofer et al., 2009, 2018; Mayer et al., 2018), no evidence exists at Karaburun for a lower NP23 low salinity event (none of the distinctive fauna and flora is noted, although sediments are of NP23 age), suggesting that connection to the World Ocean was maintained at this time, perhaps via the Çatalca Gap as suggested by Okay et al. (2019). Conversely, there is evidence for reduced surface water salinity within the NP21 portion of the Karaburun section where the nannofossil *B. bigelowii* is relatively common.

This has been regarded as a marker of reduced salinity in parts of Paratethys (Melinte-Dobrinescu and Brustur, 2008), although within NP23. However, the presence of common planktonic foraminifera within the NP21 section of Karaburun suggests surface waters were unlikely to be significantly lower than normal salinity.

Intriguingly, on the margins of the Thrace Basin, oolitic shoals occur; these shoals contain endemic Solenovian fauna (bivalves), along with sedimentary manganese ores, a typical Early Solenovian feature in eastern Paratethys (Stolyarov, 1999; Stolyarov and Ivleva, 1999). This evidence has been used by İslamoğlu et al. (2010) to suggest that during the early Solenovian (i.e. NP23), the Thrace Basin was disconnected from Tethys and only connected to eastern Paratethys. The presence of large numbers of the alga *Pediastrum* within the upper, Solenovian-equivalent, Mezardere Formation suggests a strong freshwater influence (Gürgey and Batı, 2018). Our evidence contradicts this, suggesting that a fully open marine connection existed between western Tethys and the Western Black Sea Basin within eastern Paratethys via the Çatalca Gap during NP23 (Solenovian) times, given the open marine fauna present in NP23 sediments at Karaburun and the apparently marine nature of the Mezardere Formation in the center of the Thrace Basin (Gürgey and Batı, 2018). More data on the nature of the Oligocene succession in the Thrace Basin are needed to help unravel this contradiction. We cannot absolutely exclude the possibility that the Solenovian event occurs in the NP23 stratigraphy above the highest outcrop at Karaburun, but given the thickness of the NP23 section at Karaburun and that the Solenovian event occurs in the lower part of NP23, we favor the interpretation that there is no low-salinity event recorded in the relevant stratigraphy at this locality.

9.2.3. Relative sea-level change

The progressive separation of Paratethys from Tethys which commenced around the Eocene/Oligocene boundary is often regarded as reaching an initial culmination within nannofossil Zone NP23, when Paratethys has been said to have lost its connection to the World Ocean. This Solenovian event (Popov et al., 1993, 2002, 2004; Popov and Stolyarov, 1996; Rögl, 1998; Steininger and Wessely, 2000; Sachsenhofer et al., 2018) caused the marine salinity reduction previously described and created anoxic bottom water conditions favorable for the deposition and preservation of organic-rich sediments in many parts of Paratethys (Báldi, 1984; Rögl, 1999; Schulz et al., 2004; Sachsenhofer et al., 2018). This is not observed within the Karaburun sections where sediments deposited during NP23 times represent some of the most open marine conditions based on the nature of the fossil assemblages. These sediments correspond to the flooding of the footwall and emergent and eroded Eocene reefal limestone that would have formed a paleo-topographic high. This contradicts the Paratethyan sea-level trends described by Popov et al. (2002, 2010). After a base Oligocene sea-level fall, they interpret transgression in NP22 and regression in NP23. In contrast, both Miller et al. (2005; in press) and Haq et al. (1987) indicate there might be a major eustatic transgression at the base of NP23. The Karaburun section appears to have more in common with global oceanic sea-level change than it does with local Paratethyan events, a feature that also appears to be true for the equivalent succession within the adjacent Thrace Basin (Turgut and Eseller, 2000).

Further, transgression in NP23 time is supported by aspects of data from offshore Bulgaria (Sachsenhofer et al., 2009; Mayer et al., 2018). In the well Samotino More, NP23 sediments of the Ruslar Formation (effectively a partial lateral facies equivalent of the İhsaniye Formation overlie NP20 (Late Eocene) sediments of the Avren Formation. Zones NP21 and NP22 are either highly condensed or missing by onlap, the latter suggesting a hiatus at the end of Eocene deposition, with deposition not commencing until transgression during NP23 times. Doglioni et al. (1996) observed such onlap in seismic data, while Mayer et al. (2018) demonstrate that a canyon cut offshore Bulgaria at end Eocene time is not back-filled until NP23 time. However, note that these NP23 sediments include evidence for the Solenovian reduced salinity event (the "Polbinian-type nannoflora" of Nagymarosy and Voronina (1993) and biomarker data).

9.2.4. Organic enrichment

Full details of the organic geochemistry of the İhsaniye Formation at Karaburun are presented separately (Tulan et al., 2020). In summary, it is the oldest İhsaniye Formation that is relatively, the most organic-enriched. Thus, sediments assigned to Biozone NP21 (Subzone CNO1) within the Hanging Wall Section have an average Total Organic Carbon (TOC) content of 1.45%. The richest samples are a little more than 2% TOC. They, therefore, form poor–moderate quality source rocks and with high Hydrogen Index values (140–252) suggesting they are gas-prone. Our palynology studies demonstrate a substantial input of terrestrial (type III) organic material at this stratigraphic level. Reduced bottom water oxygen levels are indicated by the presence of foraminifera such as *Hoeglundina elegans*, and this might have contributed to the preservation of organic matter.

For the Paratethys region and Thrace Basin, Oligocene stratigraphy, and the Early Oligocene specifically, often exhibits organic enrichment with rock units such the Maykop Suite, Ruslar Formation, and Mezardere Formation forming important proven or potential source rocks (Bazhenova et al., 2003; Sachsenhofer et al., 2017, 2018; Mayer et al., 2018; Gürgey and Batı, 2018).

Moreover, Sachsenhofer et al. (2018) have shown that some of the greatest organic enrichment occurs in rocks that can be assigned to biozone NP21 at the base of the Oligocene. In this sense, the organic-enrichment in the Karaburun succession fits a regional trend that includes the Alpine Foreland Basin, the Carpathians and Caucasus. This presumably relates the relative sea-level fall at or near the end of the Eocene, which would have, during lowstand, introduced both terrestrial organic matter and nutrients along the margins of Paratethys, enhancing organic productivity.

9.2.5. Regional paleogeography

The southerly connection of Eastern Paratethys with Mediterranean Tethys through the Çatalca Gap during the Early Oligocene (Okay et al., 2019) is an important element that has previously been overlooked (e.g., contrast Figure 7 with the paleogeography presented by Rögl, 1998). Karaburun would have been at the northern head of this connection (Figure 7). Our data provide support for the notion of this connection in the following ways:

- The succession is dominantly open marine and contains a diverse and often abundant fossil assemblage with planktonic foraminifera, calcareous nannofossils, and dinoflagellates all well represented. Such fossils would have needed to enter Paratethys from a connection with the World Ocean where they form typical elements of the fossil biota. Endemic species are sparse.

- The relative sea-level record appears closer to eustasy (Miller et al., in press) than the Paratethyan record (Popov et al., 2010).

- There is no evidence of a reduced salinity event in Biozone NP23 ("Solenovian" event) suggesting proximity to an oceanic connection to maintain normal salinities.

10. Summary

Rich, diverse, and well-preserved assemblages of foraminifera, calcareous nannofossils, and palynomorphs enable the stratigraphy and paleoenvironments of the Early Oligocene İhsaniye Formation exposed at Karaburun in northwest Turkey to be elucidated. It is evident that a now inverted normal fault controlled deposition (Figure 9). The underlying Late Eocene reefal limestones of the Soğucak Formation were exposed and eroded following a latest Eocene sea-level fall. Following this deposition recommenced on the hanging wall side of the fault low during the Early Oligocene (Biozone NP21, Subzone CNO1 (nannofossils), or O1 (planktonic foraminifera), although the contact between the Soğucak and oldest İhsaniye Formations is not seen, so the precise timing of the recommencement of deposition (i.e. earliest Oligocene vs latest Eocene) cannot be assessed.

The oldest approximately 20 m of the İhsaniye Formation (Biozone NP21, Subzone CNO1) is relatively enriched in organic matter (Tulan et al., 2020) and contains significant terrestrial palynomorph input and foraminiferal indicators of low oxygen bottom waters. Above this, the microfossils from the İhsaniye Formation reflect an increasingly transgressive character for approximately 35 m (Biozones NP22 – NP23, Subzone CNO3), with the footwall side of the fault transgressed by sediments that can be assigned to Biozone NP23. On the footwall side of the fault, the onset of deposition occurred within Biozone NP23 (Subzone CNO3), with the initial transgressive sediments being coarse pebbly sandstones, passing up into marls that onlap the Eocene Soğucak Formation and infill depositional depressions within it. Maximum transgression is thus within lower NP23 and is followed on the hanging wall side of the fault by a progressively shallowing-up succession of sediments displaying synsedimentary slumping and including coarse debris flows. Other than the coarse pebbly sandstone facies, most likely representative of fan delta deposition, much of the İhsaniye Formation succession at Karaburun was deposited in outer neritic–upper bathyal water depths, as determined by the foraminiferal assemblages recorded.

The open marine nature of the İhsaniye Formation succession at Karaburun contrasts with coeval Early Oligocene sediments reported from onshore and offshore Bulgaria and from the margins of the Thrace Basin. In particular, the Karaburun succession does not reflect typical Paratethyan stratigraphy that has sea-level lowering and a low salinity event ("Solenovian Event") within lower NP23 stratigraphy. The depositional pattern at Karaburun is much closer to eustatic trends (e.g. Miller, 2005; in press) that exhibit a sea-level rise culminating during NP23. On the other hand, the organic enrichment interpreted during NP21 times is a fairly typical Paratethyan feature (Sachsenhofer et al., 2018). Nonetheless, it appears that interpretation of the Karaburun stratigraphy reflects proximity to a connection to the global oceans. This might well be via the Çatalca Gap as suggested by Okay et al. (2019) (Figure 7).

Acknowledgments

Financial support for some aspects of this research was provided by the OMV Technology Development Fund. Malcolm Jones (Palynological Laboratory Services Ltd) prepared samples for palynological analysis. Sabine Gießwein from the Geological Survey of Austria made the excellent SEM photos of calcareous nannofossils. The SEM photographs of foraminifera were made using the facilities of The Natural History Museum, London. Comments by Dr Domenico Chiarella (Royal Holloway) on an early draft of the manuscript were helpful as were comments by Dr Andrew Racey on larger foraminifera encountered in the studied material. Comments by journal referees and Halliburton reviewers improved the manuscript. This paper is published with the permission of Halliburton.

References

Agnini C, Fornaciari E, Raffi I, Catanzariti R, Pälike H et al. (2014). Biozonation and biochronology of Paleogene calcareous nannofossils from low and middle latitudes. Newsletters on Stratigraphy 47/2: 131-181. doi: 10.1127/0078-0421/2014/0042

Akartuna M (1953). Geology of the Çatalca-Karaköy region. İstanbul Üniversitesi Fen Fakülesi Monografileri 13: 88 (in Turkish).

Akhmetiev MA, Popov SV, Krhovsky J, Goncharova IA, Zaporozhets NI et al. (1995). Palaeontology and stratigraphy of the Eocene – Miocene sections of the western Pre-Caucasia. Excursion guidebook: Moscow, Russian Committee for International Geological Correlation Programme.

Armstrong HA, Brasier MD (2005). Microfossils. Oxford, UK: Blackwell Publishing Ltd (Wiley-Blackwell). doi: 10.1002/9781118685440.

Aubry MP (1990). Handbook of Cenozoic Calcareous Nannoplankton. Book 4: Heliolithae (Helicoliths, Cribriliths, Lopadoliths and others). New York, NY, USA: Micropaleontology Press, The American Museum of Natural History.

Aubry MP (1992) Late Paleogene calcareous nannoplankton evolution: a tale of climatic deterioration. In: Prothero DR, Berggren WA (editors). Eocene-Oligocene Climatic and Biotic Evolution. Princeton, NJ, USA: Princeton University Press, pp. 272-309.

Aze T, Ezard, THG, Purvis A, Coxall HK, Stewart DRM et al. (2011). A phylogeny of Cenozoic macroperforate planktonic foraminifera from fossil data. Biological Reviews 86: 900-927. doi: 10.1111/j.1469-185x.2011.00178.x

Báldi T (1984). The terminal Eocene and Early Oligocene events in Hungary and the separation of an anoxic, cold Paratethys. Eclogae Geologicae Helvetiae 77: 1-27.

Bazhenova OK, Fadeeva, NP, Saint-Germes ML, Tikhomirova EE (2003). Sedimentation conditions in the eastern Paratethys Ocean in the Oligocene – Early Miocene. Moscow University Geology Bulletin 58: 11-21.

Berggren WA, Kent DV, Swisher III CC, Aubry M-P (1995). A revised Cenozoic geochronology and chronostratigraphy. In: Berggren WA, Kent DV, Hardenbol J (editors). Geochronology, Time Scales and Global Stratigraphic Correlations. SEPM Special Publication 54: 129-212.

Budilová P, Hladıkova J, Krhovsky J (1992). Late Eocene and Early Oligocene planktonic foraminifera and sediments of the Ždánice and Pozdrany Units: Carbon and oxygen isotopic study. Scripta 22: 67.

Bukry D (1974). Coccoliths as paleosalinity indicators: evidence from the Black Sea. American Association of Petroleum Geologists, Memoir 20: 303-327.

Cahuzac B, Poignant A (1997). Essai de biozonation de l'Oligo-Miocène dans le bassins européens à l'aide des grands foraminifères néritiques. Bulletin de la Société Géologique de France 168: 155-169 (in French).

Cattò S, Cavazza W, Zattin M, Okay AI (2017). No significant Alpine-age tectonic overprint of the Cimmerian Strandja Massif (SE Bulgaria and NW Turkey). International Geology Review 60: 513-529. doi: 10.1080/00206814.2017.1350604

Cavazza W, Caracciolo L, Critelli S, d'Atri A, Zuffaa GG (2013). Petrostratigraphic evolution of the Thrace Basin (Bulgaria, Greece, Turkey) within the context of Eocene-Oligocene post-collisional evolution of the Vadar-İzmir-Ankara suture zone. Geodinamica Acta 26: 27-55. doi: 10.1080/09853111.2013.858943

Colella A (1988). Pliocene-Holocene fan deltas and braid deltas in the Crati Basin, South Italy: a consequence of varying tectonic conditions. In: Nemec W, Steel RJ (editors). Fan Deltas: Sedimentology and Tectonic Settings. Glasgow, UK: Blackie & Son, pp. 50-74.

Colmenero JR, Agueda JA, Fernández LP, Salvador CI, Bahamonde JR et al. (1988). Fan-delta systems related to the Carboniferous evolution of the Cantabrian Zone, northwestern Spain. In: Nemec W, Steel RJ (editors). Fan Deltas: Sedimentology and Tectonic Settings. Glasgow, UK: Blackie & Son, 267-285.

Ćorić S, Hohenegger J (2008). Quantitative analyses of calcareous nannoplankton assemblages from the Baden-Sooss section (Middle Miocene of Vienna Basin, Austria). Geologica Carpathica 59: 447-460. doi: 10.1007/s00531-007-0287-7

Costa LI, Manum SB (1988). The description of the inter-regional zonation of the Paleogene (D1-15) and the Miocene (D16-D20). Geoligisches Jahrbuch 100: 331-339.

D'Atri A, Zuffa GG, Cavazza W, Okay AI, Di Vincenzo G (2012). Detrital supply from subduction/accretion complexes to the Eocene–Oligocene post-collisional southern Thrace Basin (NW Turkey and NE Greece). Sedimentary Geology, 243-244, 117-129. doi: 10.1016/j.sedgeo.2011.10.008

Dinu C, Wong HK, Tambrea D, Matenco L (2005). Stratigraphic and structural characteristics of the Romanian Black Sea shelf. Tectonophysics 410: 417-435. doi: 10.1016/j.tecto.2005.04.012.

Doglioni C, Busatta C, Bolis G, Marianini L, Zanella M (1996). Structural evolution of the eastern Balkans (Bulgaria). Marine and Petroleum Geology 13: 225-251.

Duman TY, Keçer M, Ateş Ş, Emre Ö, Gedik İ et al. (2004). Istanbul metropolu batısındaki (Küçükçekmece – Silivri – Çatalca yöresi) kentsel gelişme alanlarinin yer bilim verileri. Maden Tetkik ve Arama Genel Müdürlüğü, Ankara, 2 volumes, 249 pp. (in Turkish).

Eleftheriadis G, Lippold HJ (1984). Alters bestimmungen zum oligozanen Vulkanismus der Süd-Rhodopen/Nord-Griechenland. Neues Jahrbuch für Geologie und Paleontologie Monatshefte 3: 179-191 (in German).

Elmas A (2012). The Thrace Basin: stratigraphic and tectonic-palaeogeographic evolution of the Palaeogene formations of northwest Turkey. International Geology Review 54: 1419-1442. doi: 10.1080/00206814.2011.644732

Ercan A, Yağmurlu F, Uz, B (1988). Çatalca (Istanbul) yöresinde kömür içeren Tersiyer tortullarinin çökelme özellikleri ve jeofizik incelemesi. Türkiye Jeoloji Bülteni 31: 1-12 (in Turkish).

Erentöz C (1949). About the geology of the Çatalca Massif and its surroundings. İstanbul *Üniversitesi Fen Fakültesi* Mecmuası B14: 307-320 (in Turkish).

Gavrilov YO, Shchepetova EV, Shcherbinina EA, Golovanova OV, Nedumov RI et al. (2017). Sedimentary environments and geochemistry of Upper Eocene and Lower Oligocene rocks in the northeastern Caucasus. Lithology and Mineral Resources 52: 447-466. doi: 10.1134/s0024490217060037

Gedik İ, Timur E, Umut M, Bilgin AZ, Pehlivan Ş et al. (2014). Geological Map of Turkey, İstanbul F21-b, İstanbul F21c and Bursa G21-b sheets, 1:50,000 scale and explanatory text. Maden Tetkik ve Arama Genel Müdürlüğü, Ankara (in Turkish).

Görür N, Okay AI (1996). Fore-arc origin of the Thrace Basin, northwest Turkey. Geologische Rundschau 85: 662-668. doi: 10.1007/s005310050104

Gürgey K, Batı Z (2018). Palynological and petroleum geochemical assessment of the Lower Oligocene Mezardere Formation, Thrace Basin, NW Turkey. Turkish Journal of Earth Sciences 27: 349-383. doi: 10.3906/yer-1710-24

Haq BU (1980). Biogeographic history of Miocene calcareous nannoplankton and palaeoceanography of the Atlantic Ocean. Micropaleontology 26: 414-443. doi: 10.2307/1485353

Haq BU, Hardenbol J, Vail PR (1987). Chronology of fluctuating sea-levels since the Triassic (250 million years ago to present). Science 235: 1156-1167. doi: 10.1126/science.235.4793.1156

İslamoğlu Y, Harzhauser M, Gross M, Jimenez-Moreno G, Coric S et al. (2010). From Tethys to Eastern Paratethys: Oligocene depositional environments, paleoecology and paleobiogeography of the Thrace Basin (NW Turkey). International Journal of Earth Sciences 99: 183-200. doi: 21 10.1007/s00531-008-0378-0

Jones RW, Charnock MA (1985). "Morphogroups" of agglutinating Foraminifera. Their life position, feeding habits and potential applicability in (paleo) ecological studies. Revue de Paleobiologie 4: 311-320.

Jones RW, Racey A (1994). Cenozoic stratigraphy of the Arabian Peninsula and Gulf. In: Simmons MD (editor) Micropalaeontology and Hydrocarbon Exploration in the Middle East. London, UK: Chapman & Hall, pp. 273-307.

Less G, Özcan E, Okay AI (2011). Stratigraphy and Larger Foraminifera of the Middle Eocene to Lower Oligocene shallow marine units in the northern and eastern parts of the Thrace Basin, NW Turkey. Turkish Journal of Earth Sciences 20: 793-845. doi: 10.3906/yer-1010-53

Lom N, Ülgen SC, Sakinç M, Şengör AMC (2016). Geology and Stratigraphy of Istanbul region. Geodiversitas 38: 175-195. doi: 10.5252/g2016n2a3

Mackensen A, Douglas RG (1989). Down-core distribution of live and dead deep-water benthic foraminifera in box cores from the Weddell Sea and the California continental borderland, Deep Sea Research Part A. Oceanographic Research Papers 36: 879-900. doi: 10.1016/0198-0149(89)90034-4

Martini E (1971). Standard Tertiary and Quaternary calcareous nannoplankton zonation. In: Farinacci A (editor). Proceedings 2nd International Conference Planktonic Microfossils Roma: Rome (Ed. Tecnosci.) 2: 739-785.

Marzo M, Anadón P (1988). Anatomy of a conglomeratic fan-delta complex: the Eocene Montserrat Conglomerate, Ebro Basin, northeastern Spain. In: Nemec W, Steel RJ (editors). Fan Deltas: Sedimentology and Tectonic Settings. Glasgow, UK: Blackie & Son, pp. 318-340.

Mayer J, Rupprecht BJ, Sachsenhofer RF, Tari G, Bechtel A et al. (2018). Source potential and depositional environment of Oligocene and Miocene rocks offshore Bulgaria. In: Simmons MD, Tari GC, Okay AI (editors). Petroleum Geology of the Black Sea. Geological Society London Special Publications 464: 307-328. doi: 10.1144/sp464.2

Melinte-Dobrinescu M, Brustur T (2008). Oligocene – Lower Miocene events in Romania. Acta Palaeontologica Romaniae 6: 203-215.

Miller KG, Kominz MA, Browning JV, Wright JD, Mountain GS et al. (2005). The Phanerozoic record of global sea-level change. Science 310: 1293-1298. doi: 10.1126/science.1116412

Miller KG, Browning JV, Schmelz WJ, Rosenthal Y, Wright JD (In press). Cenozoic sea-level and cryospheric evolution from deep sea and continental margin records. Science Advances.

Nagymarosy A, Voronina AA (1993). Calcareous nannoplankton from the Lower Maykopian Beds (Early Oligocene, Union of Independent States). Knihovnička ZPN: 189-222.

Nakoman E (1968). Ağaçli linyitli mikroflorasinin etüdü. Türkiye Jeoloji Kurumu Bülteni 11: 68-91 (in Turkish).

Natal'in B, Say AG (2015). Eocene – Oligocene stratigraphy and structural history of the Karaburun area, southwestern Black Sea coast, Turkey: transition from extension to compression. Geological Magazine 152: 1104-1122. doi: 10.1017/s0016756815000229

Nemec W (1990). Aspects of sediment movement on steep delta slopes. In: Colella A, Prior DB (editors). Coarse-Grained Deltas. Special Publication of the International Association of Sedimentologists 10: 29-73. doi: 10.1002/9781444303858.ch3

Ní Fhlaithearta S, Reichart G-J, Jorissen FJ, Fontanier C, Rohling EJ et al. (2010). Reconstructing the seafloor environment during sapropel formation using benthic foraminiferal trace metals, stable isotopes, and sediment composition, Paleoceanography 25: PA4225. doi: 10.1029/2009PA001869.

Okada H, Bukry D (1980). Supplementary modification and introduction of code numbers to the low-latitude coccolith biostratigraphic zonation (Bukry 1973, 1975). Marine Micropaleontology 5, 321-325. doi: 10.1016/0377-8398(80)90016-x

Okada H, McInyre A (1979). Seasonal distribution of the modern Coccolithophores in the western North Atlantic Ocean. Marine Biology 54: 319-328. doi: 10.1007/bf00395438

Okay AI, Özcan E, Cavazza W, Okay N, Less G (2010). Basement types, Lower Eocene series, Upper Eocene olistostromes and the initiation of the southern Thrace Basin, NW Turkey. Turkish Journal of Earth Sciences 19: 1-25.

Okay AI, Özcan E, Hakyemez A, Siyako M, Sunal G et al. (2019). The Thrace Basin and the Black Sea: the Eocene-Oligocene marine connection. Geological Magazine 156: 39-61. doi: 10.1017/S0016756817000772

Okay AI, Satir M, Tüysüz O, Akyuz S, Chen F (2001). The tectonics of the Strandja Massif: Late Variscan and mid-Mesozoic deformation and metamorphism in the Northern Aegean. International Journal of Earth Sciences (Geologische Rundschau) 90: 217-233. doi: 10.1007/s005310000104

Okay AI, Şengör AMC, Görür N (1994). Kinematic history of the opening of the Black Sea and its effect on the surrounding regions. Geology 22: 267-270. doi: 10.1130/0091-7613(1994)022<0267:KHOTOO>2.3.CO;2

Okay AI, Simmons M, Özcan E, Starkie S, Bidgood M et al. (2020). Eocene-Oligocene succession at Kıyıköy (Midye) on the Black Sea coast in Thrace. Turkish Journal of Earth Sciences: 29: 139-153.

Oktay FY, Eren RH, Sakinç M (1992). Karaburun-Yeniköy (Istanbul) çevresinde doğu Trakya Oligosen havzasinin sedimenter jeolojisi. Proceedings of the 9th Turkish Petroleum Congress: 92-101 (in Turkish).

Özcan E, Less G, Okay AI, Báldi-Beke M, Kollányi K et al. (2010). Stratigraphy and larger foraminifera of the Eocene shallow-marine and olistostromal units of the southern part of the Thrace Basin, NW Turkey. Turkish Journal of Earth Sciences 21: 933-960.

Özcan E, Okay AI, Bürkan KA, Yücel AO, Özcan Z (2018). Middle – Late Eocene marine record of the Biga Peninsula, NW Anatolia, Turkey. Geologica Acta 16: 163-187. doi: 10.1344/GeologicaActa2018.16.2.4

Özcan E, Özcan Z, Okay AI, Akbayram K, Hakyemez A (2020). Ypresian-to Lutetian marine record in NW Turkey: a revised biostratigraphy and chronostratigraphy and implications for the Eocene paleogeography. Turkish Journal of Earth Sciences 29: 1-27.

Ozsvárt P, Kocsis L, Nyerges A, Györi O, Pálfy J (2016). The Eocene-Oligocene climate transition in the Central Paratethys. Palaeogeography, Palaeoclimatology, Palaeoecology 459: 471-487. doi: 10.1016/j.palaeo.2016.07.034

Pearson PN, Wade BS (2015). Systematic taxonomy of exceptionally well-preserved planktonic foraminifera from the Eocene/Oligocene boundary of Tanzania. Cushman Foundation for Foraminiferal Research Special Publication 45: 1-85.

Perch-Nielsen K (1985). Mesozoic calcareous nannofossils. In: Bolli HM, Saunders JB, Perch-Nielsen K, (editors) Plankton Stratigraphy. Cambridge, UK: Cambridge University Press, pp. 329-426.

Popov SV, Akhmetiev MA, Bugrova EM, Lopatin AV, Amitrov OV et al. (2002). Biogeography of the northern Peri-Tethys from the Late Eocene to the Early Miocene. Part 2. Early Oligocene. Palaeontological Journal 36 Supplement 3: S185-S259.

Popov SV, Akhmetiev MA, Zaporozhets NI, Voronina AA, Stolyarov AS (1993). Evolution of the eastern Paratethys in the Late Eocene – Early Miocene. Stratigraphy and Geological Correlation 1: 10-39.

Popov SV, Antipov MP, Zastrozhnov AS, Kurina EE, Pinchuk TN (2010). Sea-level fluctuations on the north shelf of the Eastern Paratethys in the Oligocene – Neogene. Stratigraphy and Geological Correlation 18: 200-224. doi: 10.1134/s0869593810020073

Popov SV, Ilyina LB, Nikolayeva YA (1985). Molluscs and ostracods from the Oligocene Solenovian horizon of the Eastern Paratethys. Paleont Zhurnal 1: 28-41 (In Russian).

Popov SV, Rögl F, Rozanov AY, Steininger FF, Shcherba IG, Kovac M (2004). Lithological – Paleogeographic maps of Paratethys, 10 maps Late Eocene to Pliocene. Courier Forschungsinstitut Senckenberg 250: 1-46.

Popov SV, Stolyarov AS (1996). Palaeogeography and anoxic environments of the Oligocene – Early Miocene Eastern Paratethys. Israel Journal of Earth Sciences 45: 161-167.

Popov SV, Tabachnikova IP, Bannikov AF, Sytchevskaya EK, Pinchuk TN et al. (2019). Lectostratotype of the Maikopian Group in the Belaya River section upstream of the town of Maikop (Western Ciscaucasia) in the Oligocene part. Stratigraphy and Geological Correlation 27: 339-360. doi: 10.31857/s0869-592x27370-92

Powell AJ (1982). A Stratigraphic Index of Dinoflagellate Cysts. London, UK: Chapman & Hall, p. 290.

Pross J, Houben AJ, van Simaeys S, Williams GL, Kotthoff U et al. (2010). Umbria–Marche revisited: A refined magnetostratigraphic calibration of dinoflagellate cyst events for the Oligocene of the Western Tethys. Review of Palaeobotany and Palynology 158: 213-235. doi: 10.1016/j.revpalbo.2009.09.002

Rees C, Palmer J, Palmer A (2017). Gilbert-style Pleistocene fan delta reveals tectonic development of North Island axial ranges, New Zealand. New Zealand Journal of Geology and Geophysics 61: 64-78. doi: 10.1080/00288306.2017.1406377

Rees EVL, Simmons MD, Wilson JWP (2018). Deep-water plays in the western Black Sea: insights into sediment supply within the Maykop depositional system. In: Simmons MD, Tari GC, Okay AI (editors). Petroleum Geology of the Black Sea. Geological Society, London, Special Publications 464: 247-265. doi: 10.1144/sp464.13

Rögl F (1998). Palaeogeographic considerations for Mediterranean and Paratethys seaways (Oligocene to Miocene). Annalen des Naturhistorischen Museums in Wien. Serie A für Mineralogie und Petrographie, Geologie und Paläontologie, Anthropologie und Prähistorie 99A: 279-310.

Rögl F (1999). Mediterranean and Paratethys. Facts and hypotheses of an Oligocene to Miocene Paleogeography (Short Overview). Geologica Carpathica 50: 339-349.

Rusu A (1999). Rupelian mollusk fauna of Solenovian type found in Eastern Carpathians (Romania). Acta Palaeontologica Romaniae 2: 449-452.

Sachsenhofer RF, Popov SV, Bechtel A, Ćorić S, Francu J et al. (2018). Oligocene and Lower Miocene source rocks in the Paratethys: Palaeogeographic and stratigraphic controls. In: Simmons MD, Tari GC, Okay AI (editors) Petroleum Geology of the Black Sea. Geological Society, London, Special Publications 464: 267-306. doi: 10.1144/sp464.1

Sachsenhofer RF, Stummer B, Georgiev G, Dellmour R, Bechtel A et al. (2009). Depositional environment and hydrocarbon source potential of the Oligocene Ruslar Formation (Kamchia Depression; western Black Sea). Marine and Petroleum Geology 26: 57-84. doi: 10.1016/j.marpetgeo.2007.08.004

Sachsenhofer RF, Popov SV, Akhmetiev MA, Bechtel A, Gratzer R et al. (2017). The type section of the Maikop Group (Oligocene–lower Miocene) at the Belaya River (North Caucasus): Depositional environment and hydrocarbon potential. American Association of Petroleum Geologists Bulletin 101: 289-319. doi: 10.1306/08051616027

Sahy D, Condon DJ, Hilgen FJ, Kuiper KF (2017). Reducing disparity in radio-isotopic and astrochronology-based time scales of the Late Eocene and Oligocene. Paleoceanography 32: 1018-1035. doi: 10.1002/2017pa003197

Saint-Germes ML, Bazhenova OK, Baudin F, Zaporozhets NI, Fadeeva NP (2000). Organic matter in Oligocene Maikop sequence of the North Caucasus. Lithology and Mineral Resources 35: 47-62. doi: 10.1007/bf02788284

Sakınç M (1994). Stratigraphy and paleontology of the marine Oligocene in Karaburun (west of Istanbul). Maden Tetkik ve Arama Dergisi 116: 9-14 (in Turkish).

Sancay RH, Batı Z (2020). Late Eocene to Early Oligocene palynostratigraphy of the Western Black Sea, Eastern Paratethys. Turkish Journal of Earth Sciences 29: 115-138.

Schulz H-M, Bechtel A, Rainer T, Sachsenhofer RF, Struck U (2004). Palaeoceanography of the western Central Paratethys during nannoplankton zone NP23: the Dynow Marlstone in the Austrian Molasse Basin. Geologica Carpathica 55: 311-323.

Schulz H-M, Bechtel A, Sachsenhofer RF (2005). The birth of the Paratethys during the Early Oligocene: From Tethys to an ancient Black Sea analogue? Global and Planetary Change 49: 163-176. doi: 10.1016/j.gloplacha.2005.07.001

Serra-Kiel J, Hottinger L, Caus E, Drobne K, Ferrandez C et al. (1998). Larger foraminiferal biostratigraphy of the Tethyan Paleocene and Eocene. Bulletin de la Société géologique de France 169: 281-299.

Serra-Kiel J, Gallardo-Garcia A, Razin P, Robinet J, Roger J et al. (2016). Middle Eocene – Early Miocene larger foraminifera from Dhofar (Oman) and Socotra Island (Yemen). Arab Journal of Geoscience 9: 344-439. doi: 10.1007/s12517-015-2243-3

Sheppard TH (2006). Sequence architecture of ancient rocky shorelines and their response to sea-level change: an Early Jurassic example from South Wales, UK. Journal of the Geological Society 163: 595-606. doi: 10.1144/0016-764920-015

Simmons MD, Tari GC, Okay AI (2018). Petroleum geology of the Black Sea: introduction. In: Simmons MD, Tari GC, Okay AI (editors). Petroleum Geology of the Black Sea. Geological Society, London, Special Publications 464: 1-18.

Siyako, M. (2006). Trakya havzası Tersiyer kaya birimleri. Trakya Bölgesi Litostratigrafi Birimleri'nde. Maden Tetkik ve Arama Genel Müdürlüğü, Stratigrafi Komitesi, Litostratigrafi Birimleri Serisi 2, 43-83, Ankara (in Turkish).

Siyako M, Huvaz O. (2007). Eocene stratigraphic evolution of the Thrace Basin, Turkey. Sedimentary Geology 198: 75-91. doi: 10.1016/j.sedgeo.2006.11.008

Sluijs A, Pross J, Brinkhuis H (2005). From greenhouse to icehouse; organic walled dinoflagellate cysts as paleoenvironmental indicators in the Paleogene. Earth Science Reviews 68: 281-315. doi: 10.1016/j.earscirev.2004.06.001

Steininger FF, Wessely G (1999). From the Tethyan Ocean to the Paratethys Sea: Oligocene to Neogene stratigraphy, paleogeography and paleobiogeography of the circum-Mediterranean region and the Oligocene to Neogene basin evolution in Austria. Mitteilungen der Österreichischen Geologischen Gesellschaft 92: 95-116.

Stolyarov AS (1999). Solenovian Rocks of the Lower Oligocene in the Ciscaucasia, Volga-Don, and Mangyshlak Regions (Central Part of the Eastern Paratethys): 2. Facial-Paleogeographic Deposition Environments. Lithology and Mineral Resources 34: 370-380.

Stolyarov AS, Ivleva EI (1999). Solenovian rocks of the Lower Oligocene in the Ciscaucasia, Volga-Don, and Mangyshlak Regions (central part of the Eastern Paratethys): 1. Main lithological and structural features. Lithology and Mineral Resources 34: 259-276.

Stover LE, Brinkhuis H, Damassa SP, De Verteuil L, Helby RJ et al. (1996). Mesozoic-Tertiary dinoflagellates, acritarchs and prasinophytes. In: Jansonius J, McGregor DC (editors). Palynology: Principals and Applications, 2, American Association of Stratigraphic Palynologists: 641-750.

Suc JP, Gillet H, Çağatay MN, Popescu SM, Lericolais G et al. (2015). The region of the Strandja Sill (North Turkey) and the Messinian events. Marine and Petroleum Geology 66: 149-164. doi: 10.1016/j.marpetgeo.2015.01.013

Suttill HL (2009). Sedimentological Evolution of the Emine and Kamchia Basins, Eastern Bulgaria. M.Phil. thesis, University of Edinburgh.

Tari G, Davies J, Dellmour R, Larratt E, Novotny B et al. (2009). Play types and hydrocarbon potential of the deepwater Black Sea, NE Bulgaria. The Leading Edge 28: 1076-1081. doi: 10.1190/1.3236377

Tari G, Kosi W, Fallah M, Siedl W, Kwiecinski E et al. (2014). Messinian-Style Drawdown in the Black Sea at the End Eocene. AAPG Search & Discovery Article: 90194.

Tari G, Menlikli C, Derman S (2011). Deepwater play types of the Black Sea: a brief overview. AAPG Search and Discovery Article: 10310.

Tari G, Sheya C, Calle-Bennavides L, Rosales C, Mallinson I et al. (2019). Further 2D seismic reflection evidence for a Messinian-style drawdown in the Black Sea at the end Eocene. AAPG Europe Regional Conference, Paratethys Petroleum Systems, Abstracts: 95.

Tari GC, Simmons MD (2018). History of deepwater exploration in the Black Sea and an overview of deepwater petroleum play types. In: Simmons MD, Tari GC, Okay AI (editors) Petroleum Geology of the Black Sea. Geological Society, London, Special Publications 464: 439-475. doi: 10.1144/sp464.16

Tulan E, Sachsenhofer RF, Tari G, Flecker R, Fairbank V et al. (2020). Source rock potential and depositional environment of Lower Oligocene rocks in the Karaburun area, Turkey. Turkish Journal of Earth Sciences 29: 64-84.

Turgut S, Eseller G (2000). Sequence stratigraphy, tectonics and depositional history in eastern Thrace Basin, NW Turkey. Marine and Petroleum Geology 17: 61-100. doi: 10.1016/s0264-8172(99)00015-x

Turgut S, Türkaslan M, Perinçek D (1991). Evolution of the Thrace sedimentary basin and its hydrocarbon prospectivity. In: Spencer AM (editor). Generation, Accumulation and Production of Europe's Hydrocarbons. Special Publication, European Association of Petroleum Geologists 1: 415-437. doi: 10.1016/j.sedgeo.2006.11.008

Vandenberghe N, Hilgen FJ, Speijer RP, Ogg JG, Gradstein FM et al. (2012). The Paleogene period. In: Gradstein FM, Ogg JG, Schmitz M, Ogg G (editors) .The Geologic Time Scale, Elsevier: 855-921.

van der Boon A, Beniest A, Ciurej A, Gaździcka E, Grothe A et al. (2018). The Eocene-Oligocene transition in the North Alpine Foreland Basin and subsequent closure of a Paratethys gateway. Global and Planetary Change 162: 101-119. doi: 10.1016/j.gloplacha.2017.12.009

Varol B, Baykal M, Ayyildiz T (2009). Sedimentological – stratigraphical evaluation of Tertiary carbonates (Soğucak Formation) of Thrace Basin (Bozcaada – Kıyıköy). Mineral Research and Exploration Bulletin 139: 1-5.

Vincent SJ, Kaye MND (2018). Source rock evaluation of Middle Eocene – Early Miocene mudstones from the NE margin of the Black Sea. In: Simmons MD, Tari GC, Okay AI (editors). Petroleum Geology of the Black Sea. Geological Society, London, Special Publications 464: 329-363. doi: 10.1144/sp464.7

Voronina AA, Popov SV (1984). Solenovian horizon of the Eastern Paratethys. Izvestiya Akademii Nauk SSSR, Seriya Geologicheskaya 9: 41-53 (In Russian).

Wade BS, Pearson PN, Berggren WA, Palike H (2011). Review and revision of Cenozoic tropical planktonic foraminiferal biostratigraphy and calibration to the geomagnetic polarity and astronomical time scale. Earth-Science Reviews 104, 111-142. doi: 10.1016/j.earscirev.2010.09.003

Wade BS, Olsson RK, Pearson PN, Huber BT, Berggren WA (2018). Atlas of Oligocene Planktonic Foraminifera. Cushman Foundation for Foraminiferal Research Special Publication 46: 1-524.

Wescott WA, Ethridge FG (1990). Fan deltas: alluvial fans in coastal settings. In: Rachocki AH, Church M (editors). Alluvial Fans: A Field Approach. Hoboken, NJ, USA: Wiley, pp. 195-213.

Williams GL, Brinkhuis HMAP, Pearce MA, Fensome RA, Weegink JW (2004). Southern Ocean and global dinoflagellate cyst events compared: index events for the Late Cretaceous–Neogene. Proceedings of the Ocean Drilling Program, Scientific Results 189: 1-98. doi: 10.2973/odp.proc.sr.189.107.2004

Williams GL, Bujak JP (1985). Mesozoic and Cenozoic dinoflagellates. In: Bolli HM, Saunders JB, Perch-Nielsen K (editors) Plankton Stratigraphy. Cambridge, UK: Cambridge University Press, pp. 847-964.

Williams GL, Fensome RA, Brinkhuis H, Pross J (2009). The Paleobiology of Dinoflagellates, an unpublished short text revised for the Dinoflagellate Short Course in Urbino, July 2009.

Winter A, Jordan R, Roth P (1994). Biogeography of living Coccolithophores in ocean waters. In: Winter A, Siesser W (editors): Coccolithophores. Cambridge, UK: Cambridge University Press, pp. 13-37.

Yücel AO, Özcan E, Erbil Ü (2020). Latest Priabonian larger benthic foraminiferal assemblages at the demise of the Soğucak Carbonate Platform (Thrace Basin and Black Sea shelf, NW Turkey): implications for shallow marine biostratigraphy. Turkish Journal of Earth Sciences 29: 85-114.

Yurtsever A, Çağlayan A (2002). Geological map of Turkey, sheet F21 and G21, 1:100,000 scale. Maden Tetkik ve Arama Genel Müdürlüğü, Ankara. (in Turkish)

Zaporozhets NI (1999). Palynostratigraphy and dinocyst zonation of the Middle Eocene – Lower Miocene deposits at the Belata River (Northern Caucasus). Stratigraphy and Geological Correlation 7: 161-178.

Zaporozhets NI, Akhmetiev MA (2017). Paleobotanical study of a section of the Oligocene – Lower Miocene Maikop Group along the Belaya River above the city of Maikop, Ciscaucasia. Stratigraphy and Geological Correlation 25: 638-658. doi: 10.1134/s0869593817060089